

SWASHES: a compilation of Shallow Water Analytic Solutions for Hydraulic and Environmental Studies

Complementary results

O. Delestre^{*‡,†}, C. Lucas[‡], P.-A. Ksinant^{‡,§}, F. Darboux[§],
C. Laguerre[‡], T.N.T. Vo^{‡,¶}, F. James[‡] and S. Cordier[‡]

January 18, 2016

*This document is a modified version of the published paper: **SWASHES: a compilation of Shallow Water Analytic solutions for Hydraulic and Environmental Studies**, O. Delestre, C. Lucas, P.-A. Ksinant, F. Darboux, C. Laguerre, T.-N.-T Vo, F. James, S. Cordier, International Journal for Numerical Methods in Fluids, **72(3)**: 269-300, 2013.*

Complementarily to the published version, it contains the illustration of each analytic solution, and a comparison with the numerical results obtained with FullSWOF. To help the reader, these new parts are highlighted in blue.

Abstract

Numerous codes are being developed to solve Shallow Water equations. Because there are used in hydraulic and environmental studies, their capability to simulate properly flow dynamics is critical to guarantee infrastructure and human safety. While validating these codes is an important issue, code validations are currently restricted because analytic solutions to the Shallow Water equations are rare and have been published on an individual basis over a period of more than five decades. This article aims at making analytic solutions to the Shallow Water equations easily available to code developers and users. It compiles a significant number of analytic solutions to the Shallow Water equations that are currently scattered through the literature of various scientific disciplines. The analytic solutions are described in a unified formalism to make a consistent set of test cases. These analytic solutions encompass a wide variety of flow conditions (supercritical, subcritical, shock, etc.), in 1 or 2 space dimensions, with or without rain and soil friction, for transitory flow or steady state. The corresponding source codes are made available to the community (<http://www.univ-orleans.fr/mapmo/soft/SWASHES>), so that users of Shallow Water-based models can easily find an adaptable benchmark library to validate their numerical methods.

Keywords Shallow-Water equation; Analytic solutions; Benchmarking; Validation of numerical methods; Steady-state flow; Transitory flow; Source terms

*Corresponding author: Delestre@unice.fr, presently at: Laboratoire de Mathématiques J.A. Dieudonné – Polytech Nice-Sophia , Université de Nice – Sophia Antipolis, Parc Valrose, 06108 Nice cedex 02, France

†Institut Jean le Rond d’Alembert, CNRS & UPMC Université Paris 06, UMR 7190, 4 place Jussieu, Boîte 162, F-75005 Paris, France

‡MAPMO UMR CNRS 7349, Université d’Orléans, UFR Sciences, Bâtiment de mathématiques, B.P. 6759 – F-45067 Orléans cedex 2, France

§INRA, UR 0272 Science du sol, Centre de recherche d’Orléans, CS 40001 Ardon, F-45075 Orléans cedex 2, France

¶Presently at: Department of Applied Mathematics, National University of Ireland, Galway, Republic of Ireland

1 Introduction

Shallow-Water equations have been proposed by Adh mar Barr  de Saint-Venant in 1871 to model flows in a channel [4]. Nowadays, they are widely used to model flows in various contexts, such as: overland flow [22, 47], rivers [25, 9], flooding [10, 17], dam breaks [1, 51], nearshore [6, 37], tsunami [23, 33, 41]. These equations consist in a nonlinear system of partial differential equations (PDE-s), more precisely conservation laws describing the evolution of the height and mean velocity of the fluid.

In real situations (realistic geometry, sharp spatial or temporal variations of the parameters in the model, etc.), there is no hope to solve explicitly this system of PDE-s, *i.e.* to produce analytic formul e for the solutions. It is therefore necessary to develop specific numerical methods to compute approximate solutions of such PDE-s, see for instance [49, 34, 7]. Implementation of any of such methods raises the question of the validation of the code.

Validation is an essential step to check if a model (that is the equations, the numerical methods and their implementation) suitably describes the considered phenomena. There exists at least three complementary types of numerical tests to ensure a numerical code is relevant for the considered systems of equations. First, one can produce convergence or stability results (*e.g.* by refining the mesh). This validates only the numerical method and its implementation. Second, approximate solutions can be matched to analytic solutions available for some simplified or specific cases. Finally, numerical results can be compared with experimental data, produced indoor or outdoor. This step should be done after the previous two; it is the most difficult one and must be validated by a specialist of the domain. This paper focuses on the second approach.

Analytic solutions seem underused in the validation of numerical codes, possibly for the following reasons. First, each analytic solution has a limited scope in terms of flow conditions. Second, they are currently scattered through the literature and, thus, are difficult to find. However, there exists a significant number of published analytic solutions that encompasses a wide range of flow conditions. Hence, this gives a large potential to analytic solutions for validation of numerical codes.

This work aims at overcoming these issues, on the one hand by gathering a significant set of analytic solutions, on the other hand by providing the corresponding source codes. The present paper describes the analytic solutions together with some comments about their interest and use. The source codes are made freely available to the community through the SWASHES (Shallow-Water Analytic Solutions for Hydraulic and Environmental Studies) software. The SWASHES library does not pretend to list all available analytic solutions. On the contrary, it is open for extension and we take here the opportunity to ask users to contribute to the project by sending other analytic solutions together with the dedicated code.

The paper is organized as follows: in Section 2, we briefly present the notations we use and the main properties of Shallow-Water equations. In the next two sections, we briefly outline each analytic solution. A short description of the SWASHES software can be found in Section 5. The final section is an illustration using the results of the Shallow-Water code developed by our team for a subset of analytic solutions.

2 Equations, notations and properties

First we describe the rather general settings of viscous Shallow-Water equations in two space dimensions, with topography, rain, infiltration and soil friction. In the second paragraph, we give the simplified system arising in one space dimension and recall several classical properties of the equations.

2.1 General settings

The unknowns of the equations are the water height ($h(t, x, y)$ [L]) and $u(t, x, y)$, $v(t, x, y)$ the horizontal components of the vertically averaged velocity [L/T] (Figure 1).

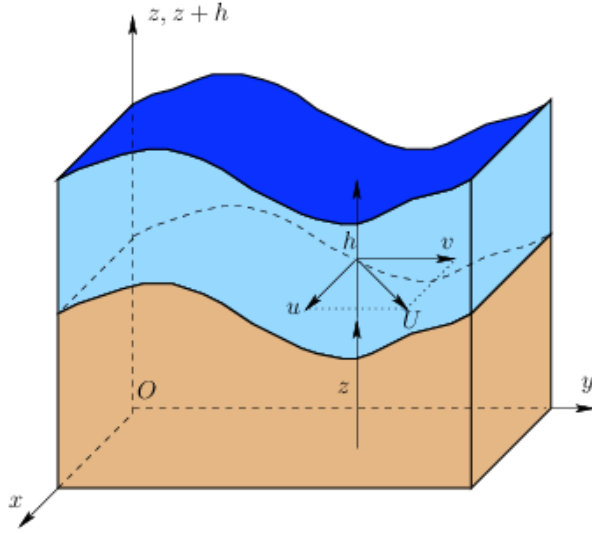


Figure 1: Notations for 2D Shallow-Water equations

The equations take the following form of balance laws, where $g = 9.81 \text{ m/s}^2$ is the gravity constant:

$$\begin{cases} \partial_t h + \partial_x(hu) + \partial_y(hv) = R - I \\ \partial_t(hu) + \partial_x\left(hu^2 + \frac{gh^2}{2}\right) + \partial_y(huv) = gh(S_{0x} - S_{f_x}) + \mu S_{dx} \\ \partial_t(hv) + \partial_x(huv) + \partial_y\left(hv^2 + \frac{gh^2}{2}\right) = gh(S_{0y} - S_{f_y}) + \mu S_{dy} \end{cases} \quad (1)$$

The first equation is actually a mass balance. The fluid density can be replaced by the height because of incompressibility. The other two equations are momentum balances, and involve forces such as gravity and friction. We give now a short description of all the terms involved, recalling the physical dimensions.

- z is the topography [L], since we consider no erosion here, it is a fixed function of space, $z(x, y)$, and we classically denote by S_{0x} (resp. S_{0y}) the opposite of the slope in the x (resp. y) direction, $S_{0x} = -\partial_x z(x, y)$ (resp. $S_{0y} = -\partial_y z(x, y)$);
- $R \geq 0$ is the rain intensity [L/T], it is a given function $R(t, x, y) \geq 0$. In this paper, it is considered uniform in space;
- I is the infiltration rate [L/T], mentioned for the sake of completeness. It is given by another model (such as Green-Ampt, Richards, etc.) and is not taken into account in the following;
- $S_f = (S_{f_x}, S_{f_y})$ is the friction force. The friction law S_f may take several forms, depending on both soil and flow properties. In the formulæ below, U is the velocity vector $U = (u, v)$ with $|U| = \sqrt{u^2 + v^2}$ and Q is the discharge $Q = (hu, hv)$. In hydrological models, two families of friction laws are encountered, based on empirical considerations. On the one hand, we have the family of Manning-Strickler's friction laws

$$S_f = C_f \frac{U|U|}{h^{4/3}} = C_f \frac{Q|Q|}{h^{10/3}}$$

$C_f = n^2$, where n is the Manning's coefficient [$\text{L}^{-1/3}\text{T}$].

On the other hand, the laws of Darcy-Weisbach's and Chézy's family writes

$$S_f = C_f \frac{U|U|}{h} = C_f \frac{Q|Q|}{h^3}.$$

With $C_f = f/(8g)$, f dimensionless coefficient, (resp. $C_f = 1/C^2$, C [$\text{L}^{1/2}/\text{T}$]) we get the Darcy-Weisbach's (resp. Chézy's) friction law. Notice that the friction may depend on the space variable, especially on large parcels. In the sequel this will not be the case.

- finally, $\mu S_d = (\mu S_{d_x}, \mu S_{d_y})$ is the viscous term with $\mu \geq 0$ the viscosity of the fluid [L^2/T].

2.2 Properties

In this section, we recall several properties of the Shallow-Water model that are useful in the flow description. For the sake of simplicity, we place ourselves in the one-dimensional case, extensions to the general setting being straightforward. The two-dimensional equations (1) rewrite

$$\begin{cases} \partial_t h + \partial_x(hu) = R - I \\ \partial_t(hu) + \partial_x\left(hu^2 + \frac{gh^2}{2}\right) = gh(S_{0x} - S_f) + \mu\partial_x(h\partial_x u) \end{cases} \quad (2)$$

The left-hand side of this system is the transport operator, corresponding to the flow of an ideal fluid in a flat channel, without friction, rain or infiltration. This is actually the model introduced by Saint-Venant in [4], and it contains several important properties of the flow. In order to emphasize these properties, we first rewrite the one-dimensional equations using vectors form:

$$\partial_t W + \partial_x F(W) = 0, \quad \text{where } W = \begin{pmatrix} h \\ hu \end{pmatrix}, \quad F(W) = \begin{pmatrix} hu \\ hu^2 + \frac{gh^2}{2} \end{pmatrix}, \quad (3)$$

with $F(W)$ the flux of the equation. The transport is more clearly evidenced in the following nonconservative form, where $A(W) = F'(W)$ is the matrix of transport coefficients:

$$\partial_t W + A(W)\partial_x W = 0, \quad A(W) = F'(W) = \begin{pmatrix} 0 & 1 \\ -u^2 + gh & 2u \end{pmatrix}. \quad (4)$$

More precisely, when $h > 0$, the matrix $A(W)$ turns out to be diagonalizable, with eigenvalues

$$\lambda_1(W) = u - \sqrt{gh} < u + \sqrt{gh} = \lambda_2(W).$$

This important property is called strict hyperbolicity (see for instance [24] and references therein for more complete information). The eigenvalues are indeed velocities, namely the ones of surface waves on the fluid, which are basic characteristics of the flow. Notice here that the eigenvalues coincide if $h = 0$ m, that is for dry zones. In that case, the system is no longer hyperbolic, and this induces difficulties at both theoretical and numerical levels. Designing numerical schemes that preserve positivity for h is very important in this context.

From these formulæ we recover a useful classification of flows, based on the relative values of the velocities of the fluid, u , and of the waves, \sqrt{gh} . Indeed if $|u| < \sqrt{gh}$ the characteristic velocities have opposite signs, and information propagate upward as well as downward the flow, which is then said subcritical or fluvial. On the other hand, when $|u| > \sqrt{gh}$, the flow is supercritical, or torrential, all the information go downwards. A transcritical regime exists when some parts of a flow are subcritical, other supercritical.

Since we have two unknowns h and u (or equivalently h and $q = hu$), a subcritical flow is therefore determined by one upstream and one downstream value, whereas a supercritical flow is completely determined by the two upstream values. Thus for numerical simulations, we have to impose one variable for

subcritical inflow/outflow. We impose both variables for supercritical inflow and for supercritical outflow, free boundary conditions are considered (see for example [8]).

In this context, two quantities are useful. The first one is a dimensionless parameter called the Froude number

$$\text{Fr} = \frac{|u|}{\sqrt{gh}}. \quad (5)$$

It is the analogue of the Mach number in gas dynamics, and the flow is subcritical (resp. supercritical) if $\text{Fr} < 1$ (resp. $\text{Fr} > 1$). The other important quantity is the so-called critical height h_c which writes

$$h_c = \left(\frac{q}{\sqrt{g}} \right)^{2/3}, \quad (6)$$

for a given discharge $q = hu$. It is a very readable criterion for criticality: the flow is subcritical (resp. supercritical) if $h > h_c$ (resp. $h < h_c$).

When additional terms are present, other properties have to be considered, for instance the occurrence of steady states (or equilibrium) solutions. These specific flows are defined and discussed in Section 3.

3 Steady state solutions

In this section, we focus on a family of steady state solutions, that is solutions that satisfy:

$$\partial_t h = \partial_t u = 0.$$

Replacing this relation in the one-dimensional Shallow-Water equations (2), the mass equation gives $\partial_x(hu) = R$ or $hu = q = Rx + q_0$, where $q_0 = q(t, x = 0)$. Similarly the momentum equation writes

$$\partial_x \left(\frac{q^2}{h} + \frac{gh^2}{2} \right) = -gh\partial_x z - ghS_f(h, q) + \mu\partial_x \left(h\partial_x \frac{q}{h} \right).$$

Thus for $h \neq 0$, we have the following system

$$\begin{cases} q = Rx + q_0, \\ \partial_x z = \frac{1}{gh} \left(\frac{q^2}{h^2} - gh \right) \partial_x h - S_f(h, q) + \frac{\mu}{gh} \partial_x \left(h\partial_x \frac{q}{h} \right). \end{cases} \quad (7)$$

System (7) is the key point of the following series of analytic solutions. For these solutions, the strategy consists in choosing either a topography and getting the associated water height or a water height and deducing the associated topography.

Since [5], it is well known that the source term treatment is a crucial point in preserving steady states. With the following steady states solutions, one can check if the steady state at rest and dynamic steady states are satisfied by the considered schemes using various flow conditions (fluvial, torrential, transcritical, with shock, etc.). Moreover, the variety of inflow and outflow configurations (flat bottom/varying topography, with/without friction, etc.) gives a validation of boundary conditions treatment. One must note that, as different source terms (topography, friction, rain and diffusion) are taken into account, these solutions can also validate the source terms treatment.

The last remark deals with initial conditions: if initial conditions are taken equal to the solution at the steady state, one can only conclude on the ability of the numerical scheme to *preserve* steady states. In order to prove the capacity to *catch* these states, initial conditions should be different from the steady state. This is the reason why the initial conditions, as well as the boundary conditions, are described in each case.

Table 1 lists all steady-state solutions available in SWASHES and outlines their main features.

Steady-state solutions		Flow criticality				Friction			Comments	
		Sub.	Sup.	Sub.→Sup.	Jump	Man.	D.-W.	Other		Null
Bumps	Lake at rest with immersed bump	3.1.1	[16]						X	Hydrostatic equilibria
	Lake at rest with emerged bump	3.1.2	[16]							Hydrostatic equilibria and wet-dry transition
	Subcritical flow	3.1.3	[27]	X						Initially steady state at rest
	Transcritical flow without shock	3.1.4	[27]		X					Initially steady state at rest
	Transcritical flow with shock	3.1.5	[27]			X				Initially steady state at rest
	Long channel with subcritical flow	3.2.1	[53]	X			X			Initially dry channel. 1000 m long
	Long channel with supercritical flow	3.2.1	[16]		X		X			Initially dry channel. 1000 m long
	Long channel with sub- to super-critical flow	3.2.1	[53]		X		X			Initially dry channel. 1000 m long
	Long channel with super- to sub-critical flow	3.2.1	[53]			X	X			Initially dry channel. 1000 m long
	Short channel with smooth transition and shock	3.2.2	[53]		X		X			At $t=0$, lake downstream. 100 m long
	Short channel with supercritical flow	3.2.2	[16]			X				Initially dry. 100 m long
	Short channel with sub- to super-critical flow	3.2.2	[53]				X			At $t=0$, lake downstream. 100 m long
	Very long, undulating and periodic channel with subcritical flow	3.2.3	[53]	X						At $t=0$, lake downstream. 5000 m long
	Rain on a long channel with subcritical flow	3.3.1	[53]	X			X			Initially dry. 1000 m long
	Rain on a long channel with supercritical flow	3.3.2	[53]		X		X			Initially dry. 1000 m long
Long channel with subcritical flow and diffusion	3.4.1	[19]	X				X		Initially dry. 1000 m long	
Long channel with supercritical flow and diffusion	3.4.2	[19]		X				X	Initially dry. 1000 m long	
Pseudo-2D short channel with subcritical flow	3.5.1	[35]	X			X			Rectangular cross section. Initially dry. 200 m long	
Pseudo-2D short channel with supercritical flow	3.5.2	[35]		X			X		Rectangular cross section. Initially wet. 200 m long	
Pseudo-2D short channel with smooth transition	3.5.3	[35]			X				Rectangular cross section. Initially partly-wet. 200 m long	
Pseudo-2D short channel with shock	3.5.4	[35]				X			Rectangular cross section. Initially dry. 200 m long	
Pseudo-2D long channel with subcritical flow	3.5.5	[35]	X						Isoscele trapezoidal cross section. Initially dry. 400 m long	
Pseudo-2D long channel with smooth transition and shock	3.5.6	[35]			X				Isoscele trapezoidal cross section. Initially dry. 400 m long	

Slope is always variable. Sub.: Subcritical; Sup.: Supercritical; Man.: Manning; D.-W.: Darcy-Weisbach

Table 1: Analytic solutions for shallow flow equations and their main features — Steady-state cases

3.1 Bumps

Here we present a series of steady state cases proposed in [27, p.14-17] based on an idea introduced in [32], with a flat topography at the boundaries, no rain, no friction and no diffusion ($R = 0$ m/s, $S_f = 0$ and $\mu = 0$ m²/s). Thus system (7) reduces to

$$\begin{cases} q = q_0, \\ \partial_x z = \frac{1}{gh} \left(\frac{q^2}{h^2} - gh \right) \partial_x h. \end{cases}$$

In the case of a regular solution, we get the Bernoulli relation

$$\frac{q_0^2}{2gh^2(x)} + h(x) + z(x) = Cst \quad (8)$$

which gives us the link between the topography and the water height. Initial conditions satisfy the hydrostatic equilibrium

$$h + z = Cst \text{ and } q = 0 \text{ m}^2/\text{s}. \quad (9)$$

These solutions test the preservation of steady states and the boundary conditions treatment.

In the following cases, we choose a domain of length $L = 25$ m with a topography given by:

$$z(x) = \begin{cases} 0.2 - 0.05(x - 10)^2 & \text{if } 8 \text{ m} < x < 12 \text{ m}, \\ 0 & \text{else.} \end{cases}$$

3.1.1 Lake at rest with an immersed bump

In the case of a lake at rest with an immersed bump, the water height is such that the topography is totally immersed [16]. In such a configuration, starting from the steady state, the velocity must be null and the water surface should stay flat.

In SWASHES we have the following initial conditions:

$$h + z = 0.5 \text{ m and } q = 0 \text{ m}^2/\text{s}$$

and the boundary conditions

$$\begin{cases} h = 0.5 \text{ m}, \\ q = 0 \text{ m}^2/\text{s}. \end{cases}$$

3.1.2 Lake at rest with an emerged bump

The case of a lake at rest with an emerged bump is the same as in the previous section except that the water height is smaller in order to have emergence of some parts of the topography [16]. Here again, we initialize the solution at steady state and the solution is null velocity and flat water surface.

In SWASHES we consider the following initial conditions:

$$h + z = \max(0.1, z) \text{ m and } q = 0 \text{ m}^2/\text{s}$$

and the boundary conditions

$$\begin{cases} h = 0.1 \text{ m}, \\ q = 0 \text{ m}^2/\text{s}. \end{cases}$$

3.1.3 Subcritical flow

After testing the two steady states at rest, the user can increase the difficulty with dynamical steady states. In the case of a subcritical flow, using (8), the water height is given by the resolution of

$$h(x)^3 + \left(z(x) - \frac{q_0^2}{2gh_L^2} - h_L \right) h(x)^2 + \frac{q_0^2}{2g} = 0, \quad \forall x \in [0, L],$$

where $h_L = h(x = L)$.

Thanks to the Bernoulli relation (8), we can notice that the water height is constant when the topography is constant, decreases (respectively increases) when the bed slope increases (resp. decreases). The water height reaches its minimum at the top of the bump [27].

In SWASHES, the initial conditions are

$$h + z = 2 \text{ m and } q = 0 \text{ m}^2/\text{s}$$

and the boundary conditions are chosen as

$$\begin{cases} \text{upstream: } q = 4.42 \text{ m}^2/\text{s}, \\ \text{downstream: } h = 2 \text{ m}. \end{cases}$$

3.1.4 Transcritical flow without shock

In this part, we consider the case of a transcritical flow, without shock [27]. Again thanks to (8), we can express the water height as the solution of

$$h(x)^3 + \left(z(x) - \frac{q_0^2}{2gh_c^2} - h_c - z_M \right) h(x)^2 + \frac{q_0^2}{2g} = 0, \quad \forall x \in [0, L],$$

where $z_M = \max_{x \in [0, L]} z$ and h_c is the corresponding water height.

The flow is fluvial upstream and becomes torrential at the top of the bump.

Initial conditions can be taken equal to

$$h + z = 0.66 \text{ m and } q = 0 \text{ m}^2/\text{s}$$

and for the boundary conditions

$$\begin{cases} \text{upstream: } q = 1.53 \text{ m}^2/\text{s}, \\ \text{downstream: } h = 0.66 \text{ m while the flow is subcritical.} \end{cases}$$

3.1.5 Transcritical flow with shock

If there is a shock in the solution [27], using (8), the water height is given by the resolution of

$$\begin{cases} h(x)^3 + \left(z(x) - \frac{q_0^2}{2gh_c^2} - h_c - z_M \right) h(x)^2 + \frac{q_0^2}{2g} = 0 & \text{for } x < x_{shock}, \\ h(x)^3 + \left(z(x) - \frac{q_0^2}{2gh_L^2} - h_L \right) h(x)^2 + \frac{q_0^2}{2g} = 0 & \text{for } x > x_{shock}, \\ q_0^2 \left(\frac{1}{h_1} - \frac{1}{h_2} \right) + \frac{g}{2} (h_1^2 - h_2^2) = 0. \end{cases} \quad (10)$$

In these equalities, $z_M = \max_{x \in [0, L]} z$, h_c is the corresponding water height, $h_L = h(x = L)$ and $h_1 = h(x_{shock}^-)$, $h_2 = h(x_{shock}^+)$ are the water heights upstream and downstream respectively. The shock

is located thanks to the third relation in system (10), which is a Rankine-Hugoniot's relation.

As for the previous case, the flow becomes supercritical at the top of the bump but it becomes again fluvial after a hydraulic jump.

One can choose for initial conditions

$$h + z = 0.33 \text{ m and } q = 0 \text{ m}^2/\text{s}$$

and the following boundary conditions

$$\begin{cases} \text{upstream: } q = 0.18 \text{ m}^2/\text{s}, \\ \text{downstream: } h = 0.33 \text{ m}. \end{cases}$$

We can find a generalisation of this case with a friction term in Hervouet's work [31].

3.2 Mac Donald's type 1D solutions

Following the lines of [35, 36], we give here some steady state solutions of system (2) with varying topography and friction term (from [53, 16]). Rain and diffusion are not considered ($R = 0 \text{ m/s}$, $\mu = 0 \text{ m}^2/\text{s}$), so the steady states system (7) reduces to

$$\partial_x z = \left(\frac{q^2}{gh^3} - 1 \right) \partial_x h - S_f. \quad (11)$$

From this relation, one can make as many solutions as required. In this section, we present some of them that are obtained for specific values of the length L of the domain, and for fixed parameters (such as the friction law and its coefficient). The water height profile and the discharge are given, and we compute the corresponding topographies solving equation (11). We have to mention that there exists another approach, classical in hydraulics. It consists in considering a given topography and a discharge. From these, the steady-state water height is deduced thanks to equation (11) and to the classification of water surface profiles (see among others [14] and [30]). Solutions obtained using this approach may be found in [56] for example. Finally, note that some simple choices for the free surface may lead to exact analytic solutions.

The solutions given in this section are more intricate than the ones of the previous section, as the topography can vary near the boundary. Consequently they give a better validation of the boundary conditions. If $S_f \neq 0$ (we have friction at the bottom), the following solutions can prove if the friction terms are coded in order to satisfy the steady states.

Remark 1 *All these solutions are given by the numerical resolution of an equation. So, the space step should be small enough to have a sufficiently precise solution. It means that the space step used to get these solutions should be smaller than the space step of the code to be validated.*

3.2.1 Long channel: 1000 m

Subcritical case We consider a 1000 m long channel with a discharge of $q = 2 \text{ m}^2/\text{s}$ [53]. The flow is constant at inflow and the water height is prescribed at outflow, with the following values:

$$\begin{cases} \text{upstream: } q = 2 \text{ m}^2/\text{s}, \\ \text{downstream: } h = h_{ex}(1000). \end{cases}$$

The channel is initially dry, *i.e.* initial conditions are

$$h = 0 \text{ m and } q = 0 \text{ m}^2/\text{s}.$$

The water height is given by

$$h_{ex}(x) = \left(\frac{4}{g} \right)^{1/3} \left(1 + \frac{1}{2} \exp \left(-16 \left(\frac{x}{1000} - \frac{1}{2} \right)^2 \right) \right). \quad (12)$$

We remind the reader that $q = 2 \text{ m}^2/\text{s}$ on the domain and that the topography is calculated iteratively thanks to (11). We can consider the two friction laws explained in the introduction, with the coefficients $n = 0.033 \text{ m}^{-1/3}\text{s}$ for Manning's and $f = 0.093$ for Darcy-Weisbach's. Under such conditions, we get a subcritical steady flow.

Supercritical case We still consider a 1000 m long channel, but with a constant discharge $q = 2.5 \text{ m}^2/\text{s}$ on the whole domain [16]. The flow is supercritical both at inflow and at outflow, thus we consider the following boundary conditions:

$$\begin{cases} \text{upstream: } q = 2.5 \text{ m}^2/\text{s} \text{ and } h = h_{ex}(0), \\ \text{downstream: free.} \end{cases}$$

The initial conditions are a dry channel

$$h = 0 \text{ m} \text{ and } q = 0 \text{ m}^2/\text{s}.$$

With the water height given by

$$h_{ex}(x) = \left(\frac{4}{g}\right)^{1/3} \left(1 - \frac{1}{5} \exp\left(-36 \left(\frac{x}{1000} - \frac{1}{2}\right)^2\right)\right) \quad (13)$$

and the friction coefficients equal to $n = 0.04 \text{ m}^{-1/3}\text{s}$ for Manning's and $f = 0.065$ for Darcy-Weisbach's friction law, the flow is supercritical.

Subcritical-to-supercritical case The channel is 1000 m long and the discharge at equilibrium is $q = 2 \text{ m}^2/\text{s}$ [53]. The flow is subcritical upstream and supercritical downstream, thus we consider the following boundary conditions:

$$\begin{cases} \text{upstream: } q = 2 \text{ m}^2/\text{s}, \\ \text{downstream: free.} \end{cases}$$

As initial conditions, we consider a dry channel

$$h = 0 \text{ m} \text{ and } q = 0 \text{ m}^2/\text{s}.$$

In this configuration, the water height is

$$h_{ex}(x) = \begin{cases} \left(\frac{4}{g}\right)^{1/3} \left(1 - \frac{1}{3} \tanh\left(3 \left(\frac{x}{1000} - \frac{1}{2}\right)\right)\right) & \text{for } 0 \text{ m} \leq x \leq 500 \text{ m}, \\ \left(\frac{4}{g}\right)^{1/3} \left(1 - \frac{1}{6} \tanh\left(6 \left(\frac{x}{1000} - \frac{1}{2}\right)\right)\right) & \text{for } 500 \text{ m} < x \leq 1000 \text{ m}, \end{cases}$$

with a friction coefficient $n = 0.0218 \text{ m}^{-1/3}\text{s}$ (resp. $f = 0.042$) for the Manning's (resp. the Darcy-Weisbach's) law. Thus we get a transcritical flow (from fluvial to torrential via a transonic point).

Supercritical-to-subcritical case As in the previous cases, the domain is 1000 m long and the discharge is $q = 2 \text{ m}^2/\text{s}$ [53]. The boundary conditions are a torrential inflow and a fluvial outflow:

$$\begin{cases} \text{upstream: } q = 2 \text{ m}^2/\text{s} \text{ and } h = h_{ex}(0), \\ \text{downstream: } h = h_{ex}(1000). \end{cases}$$

At time $t = 0 \text{ s}$, the channel is initially dry

$$h = 0 \text{ m} \text{ and } q = 0 \text{ m}^2/\text{s}.$$

The water height is defined by the following discontinuous function

$$h_{ex}(x) = \begin{cases} \left(\frac{4}{g}\right)^{1/3} \left(\frac{9}{10} - \frac{1}{6} \exp\left(-\frac{x}{250}\right)\right) & \text{for } 0 \text{ m} \leq x \leq 500 \text{ m}, \\ \left(\frac{4}{g}\right)^{1/3} \left(1 + \sum_{k=1}^3 a_k \exp\left(-20k \left(\frac{x}{1000} - \frac{1}{2}\right)\right) + \frac{4}{5} \exp\left(\frac{x}{1000} - 1\right)\right) & \text{for } 500 \text{ m} \leq x \leq 1000 \text{ m}, \end{cases}$$

with $a_1 = -0.348427$, $a_2 = 0.552264$, $a_3 = -0.55558$.

The friction coefficients are $n = 0.0218 \text{ m}^{-1/3}\text{s}$ for the Manning's law and $f = 0.0425$ for the Darcy-Weisbach's law. The steady state solution is supercritical upstream and becomes subcritical through a hydraulic jump located at $x = 500 \text{ m}$.

3.2.2 Short channel: 100 m

In this part, the friction law we consider is the Manning's law. Generalization to other classical friction laws is straightforward.

Case with smooth transition and shock The length of the channel is 100 m and the discharge at steady states is $q = 2 \text{ m}^2/\text{s}$ [53]. The flow is fluvial both upstream and downstream, the boundary conditions are fixed as follows

$$\begin{cases} \text{upstream: } q = 2 \text{ m}^2/\text{s}, \\ \text{downstream: } h = h_{ex}(100). \end{cases}$$

To have a case including two kinds of flow (subcritical and supercritical) and two kinds of transition (transonic and shock), we consider a channel filled with water, *i.e.*

$$h(x) = \max(h_{ex}(100) + z(100) - z(x), 0) \text{ and } q = 0 \text{ m}^2/\text{s}.$$

The water height function has the following formula

$$h_{ex}(x) = \begin{cases} \left(\frac{4}{g}\right)^{1/3} \left(\frac{4}{3} - \frac{x}{100}\right) - \frac{9x}{1000} \left(\frac{x}{100} - \frac{2}{3}\right) & \text{for } 0 \text{ m} \leq x \leq \frac{200}{3} \approx 66.67 \text{ m}, \\ \left(\frac{4}{g}\right)^{1/3} \left(a_1 \left(\frac{x}{100} - \frac{2}{3}\right)^4 + a_1 \left(\frac{x}{100} - \frac{2}{3}\right)^3 - a_2 \left(\frac{x}{100} - \frac{2}{3}\right)^2 + a_3 \left(\frac{x}{100} - \frac{2}{3}\right) + a_4\right) & \text{for } \frac{200}{3} \approx 66.67 \text{ m} \leq x \leq 100 \text{ m}, \end{cases}$$

with $a_1 = 0.674202$, $a_2 = 21.7112$, $a_3 = 14.492$ et $a_4 = 1.4305$.

In this case, the Manning's friction coefficient is $n = 0.0328 \text{ m}^{-1/3}\text{s}$, the inflow is subcritical, becomes supercritical via a sonic point, and, through a shock (located at $x = 200/3 \approx 66.67 \text{ m}$), becomes subcritical again.

Supercritical case The channel we consider is still 100 m long and the equilibrium discharge is $q = 2 \text{ m}^2/\text{s}$ [16]. The flow is torrential at the bounds of the channel, thus the boundary conditions are

$$\begin{cases} \text{upstream: } q = 2 \text{ m}^2/\text{s} \text{ and } h = h_{ex}(0), \\ \text{downstream: free.} \end{cases}$$

As initial conditions, we consider an empty channel which writes

$$h = 0 \text{ m} \quad \text{and} \quad q = 0 \text{ m}^2/\text{s}.$$

The water height is given by

$$h_{ex}(x) = \left(\frac{4}{g}\right)^{1/3} \left(1 - \frac{1}{4} \exp\left(-4 \left(\frac{x}{100} - \frac{1}{2}\right)^2\right)\right)$$

and the friction coefficient is $n = 0.03 \text{ m}^{-1/3}\text{s}$ (for the Manning's law). The flow is entirely torrential.

Subcritical-to-supercritical case A 100 m long channel has a discharge of $q = 2 \text{ m}^2/\text{s}$ [53]. The flow is fluvial at inflow and torrential at outflow with following boundary conditions

$$\begin{cases} \text{upstream: } q = 2 \text{ m}^2/\text{s}, \\ \text{downstream: free.} \end{cases}$$

As in the subcritical case, the initial condition is an empty channel with a puddle downstream

$$h(x) = \max(h_{ex}(100) + z(100) - z(x), 0) \quad \text{and} \quad q = 0 \text{ m}^2/\text{s},$$

and the water height is

$$h_{ex}(x) = \left(\frac{4}{g}\right)^{1/3} \left(1 - \frac{(x-50)}{200} + \frac{(x-50)^2}{30000}\right).$$

The Manning's friction coefficient for the channel is $n = 0.0328 \text{ m}^{-1/3}\text{s}$. We get a transcritical flow: subcritical upstream and supercritical downstream.

3.2.3 Long channel: 5000 m, periodic and subcritical

For this case, the channel is much longer than for the previous ones: 5000 m, but the discharge at equilibrium is still $q = 2 \text{ m}^2/\text{s}$ [53]. Inflow and outflow are both subcritical. The boundary conditions are taken as:

$$\begin{cases} \text{upstream: } q = 2 \text{ m}^2/\text{s}, \\ \text{downstream: } h = h_{ex}(5000). \end{cases}$$

We consider a dry channel with a little lake at rest downstream as initial conditions:

$$h(x) = \max(h_{ex}(5000) + z(5000) - z(x), 0) \quad \text{and} \quad q = 0 \text{ m}^2/\text{s}.$$

We take the water height at equilibrium as a periodic function in space, namely

$$h_{ex}(x) = \frac{9}{8} + \frac{1}{4} \sin\left(\frac{\pi x}{500}\right)$$

and the Manning's constant is $n = 0.03 \text{ m}^{-1/3}\text{s}$. We get a subcritical flow. As the water height is periodic, the associated topography (solution of Equation (11)) is periodic as well: we get a periodic configuration closed to the ridges-and-furrows configuration. Thus this case is interesting for the validation of numerical methods for overland flow simulations on agricultural fields.

3.3 Mac Donald's type 1D solutions with rain

In this section, we consider the Shallow Water system (2) with rain (but without viscosity: $\mu = 0 \text{ m}^2/\text{s}$) at steady states [53]. The rain intensity is constant, equal to R_0 . The rain is uniform on the domain $[0, L]$. Under these conditions, if we denote by q_0 the discharge value at inflow $q(t, 0) = q_0$, we have:

$$q(x) = q_0 + xR_0, \quad \text{for } 0 \leq x \leq L. \quad (14)$$

The solutions are the same as in Section 3.2, except that the discharge is given by (14). But the rain term modifies the expression of the topography through a new rain term as written in (7). More precisely, Equation (11) is replaced by

$$\partial_x z = \left(\frac{q^2}{gh^3} - 1 \right) \partial_x h - \frac{2qR_0}{gh^2} - S_f.$$

These solutions allow the validation of the numerical treatment of the rain. Remark 1, mentioned in the previous section, applies to these solutions too.

3.3.1 Subcritical case for a long channel

For a 1000 m long channel, we consider a flow which is fluvial on the whole domain. Thus we impose the following boundary conditions:

$$\begin{cases} \text{upstream: } q = q_0, \\ \text{downstream: } h = h_{ex}(1000), \end{cases}$$

with the initial conditions

$$h = 0 \text{ m and } q = 0 \text{ m}^2/\text{s},$$

where h_{ex} is the water height at steady state given by (12).

In SWASHES, for the friction term, we can choose either Manning's law with $n = 0.033 \text{ m}^{-1/3}\text{s}$ or Darcy-Weisbach's law with $f = 0.093$, the discharge q_0 is fixed at $1 \text{ m}^2/\text{s}$ and the rain intensity is $R_0 = 0.001 \text{ m/s}$.

3.3.2 Supercritical case for a long channel

The channel length remains unchanged (1000 m), but, as the flow is supercritical, the boundary conditions are

$$\begin{cases} \text{upstream: } q = q_0 \text{ and } h = h_{ex}(0), \\ \text{downstream: free.} \end{cases}$$

At initial time, the channel is dry

$$h = 0 \text{ m and } q = 0 \text{ m}^2/\text{s}.$$

At steady state, the formula for the water height is (13).

From a numerical point of view, for this case, we recommend that the rain does not start at the initial time. The general form of the recommended rainfall event is

$$R(t) = \begin{cases} 0 \text{ m/s} & \text{if } t < t_R, \\ R_0 & \text{else,} \end{cases}$$

with $t_R = 1500 \text{ s}$. Indeed, this allows to get two successive steady states: for the first one the discharge is constant in space q_0 and for the second one the discharge is (14) with the chosen height profile (13).

In SWASHES, we have a friction coefficient $n = 0.04 \text{ m}^{-1/3}\text{s}$ for Manning's law, $f = 0.065$ for Darcy-Weisbach's law. Inflow discharge is $q_0 = 2.5 \text{ m}^2/\text{s}$ and $R_0 = 0.001 \text{ m/s}$.

3.4 Mac Donald's type 1D solutions with diffusion

Following the lines of [35, 36], Delestre and Marche, in [19], proposed new analytic solutions with a diffusion term (with $R = 0 \text{ m/s}$). To our knowledge, these are the only analytic solutions available in the literature with a diffusion source term. In [19], the authors considered system (2) with the source terms derived in [38], *i.e.*:

$$S_f = \frac{1}{g} \left(\frac{\alpha_0(h)}{h} u + \alpha_1(h) |u|u \right) \quad \text{and} \quad \mu = 4\mu_h$$

with

$$\alpha_0(h) = \frac{k_l}{1 + \frac{k_l h}{3\mu_v}} \quad \text{and} \quad \alpha_1(h) = \frac{k_t}{\left(1 + \frac{k_l h}{3\mu_v}\right)^2}$$

where μ_v [T] (respectively μ_h [L²/T]) is the vertical (resp. the horizontal) eddy viscosity and k_l [T/L] (resp. k_t [1/L]) the laminar (resp. the turbulent) friction coefficient. At steady states we recover (7) with $R = 0$ m/s, or again

$$\begin{cases} q = q_0, \\ \partial_x z = \frac{1}{gh} \left(\frac{q^2}{h^2} - gh \right) \partial_x h - S_f(h, q) + \frac{\mu}{gh^2} \left(-q \partial_{xx} h + \frac{q}{h} (\partial_x h)^2 \right). \end{cases} \quad (15)$$

As for the previous cases, the topography is evaluated thanks to the momentum equation of (15).

These cases allow for the validation of the diffusion source term treatment. These solutions may be easily adapted to Manning's and Darcy-Weisbach's friction terms. Remark 1 applies to these solutions too.

In [19], the effect of μ_h , μ_v , k_t and k_l is studied by using several values. In what follows, we present only two of these solutions: a subcritical flow and a supercritical flow.

3.4.1 Subcritical case for a long channel

A 1000 m long channel has a discharge of $q = 1.5$ m²/s. The flow is fluvial at both channel boundaries, thus the boundary conditions are:

$$\begin{cases} \text{upstream: } q = 1.5 \text{ m}^2/\text{s}, \\ \text{downstream: } h = h_{ex}(1000). \end{cases}$$

The channel is initially dry

$$h = 0 \text{ m} \quad \text{and} \quad q = 0 \text{ m}^2/\text{s}$$

and the water height at steady state (h_{ex}) is the same as in Section 3.2.1.

In SWASHES, the parameters are: $k_t = 0.01$, $k_l = 0.001$, $\mu_v = 0.01$ and $\mu_h = 0.001$.

3.4.2 Supercritical case for a long channel

We still consider a 1000 m long channel, with a constant discharge $q = 2.5$ m²/s on the whole domain. Inflow and outflow are both torrential, thus we choose the following boundary conditions:

$$\begin{cases} \text{upstream: } q = 2.5 \text{ m}^2/\text{s} \text{ and } h = h_{ex}(0), \\ \text{downstream: free.} \end{cases}$$

We consider a dry channel as initial condition:

$$h = 0 \text{ m} \text{ and } q = 0 \text{ m}^2/\text{s}.$$

The water height h_{ex} at steady state is given by function (13).

In SWASHES, we have: $k_t = 0.005$, $k_l = 0.001$, $\mu_v = 0.01$ and $\mu_h = 0.1$.

3.5 Mac Donald pseudo-2D solutions

In this section, we give several analytic solutions for the pseudo-2D Shallow-Water system. This system can be considered as an intermediate between the one-dimensional and the two-dimensional models. More precisely, these equations model a flow in a rectilinear three-dimensional channel with the quantities averaged not only on the vertical direction but also on the width of the channel. For the derivation, see for example [26]. Remark 1, mentioned for Mac Donald's type 1D solutions, applies to these pseudo-2D solutions too.

We consider six cases for non-prismatic channels introduced in [35]. These channels have a variable slope and their width is also variable in space. More precisely, each channel is determined through the definition of the bottom width B (as a function of the space variable x) and the slope of the boundary Z (Figure 2). The bed slope is an explicit function of the water height, detailed in the following.

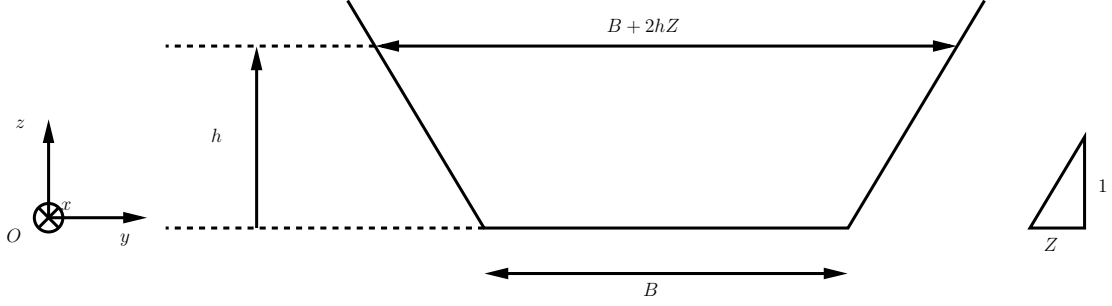


Figure 2: Notations for the Mac Donald pseudo-2D solutions

Solution	B (m)	Z (m)	L (m)	h_{in} (m)	h_{out} (m)
Subcritical flow in a short domain	$B_1(x)$	0	200		0.902921
Supercritical flow in a short domain	$B_1(x)$	0	200	0.503369	
Smooth transition in a short domain	$B_1(x)$	0	200		
Hydraulic jump in a short domain	$B_1(x)$	0	200	0.7	1.215485
Subcritical flow in a long domain	$B_2(x)$	2	400		0.904094
Smooth transition followed by a hydraulic jump in a long domain	$B_2(x)$	2	400		1.2

Table 2: Main features of the cases of pseudo-2D channels

The features of these cases are summarized in table 2. In this table, the functions for the bed shape are:

$$B_1(x) = 10 - 5 \exp \left(-10 \left(\frac{x}{200} - \frac{1}{2} \right)^2 \right) \text{ for } 0 \text{ m} \leq x \leq L = 200 \text{ m} ,$$

$$B_2(x) = 10 - 5 \exp \left(-50 \left(\frac{x}{400} - \frac{1}{3} \right)^2 \right) - 5 \exp \left(-50 \left(\frac{x}{400} - \frac{2}{3} \right)^2 \right) \text{ for } 0 \text{ m} \leq x \leq L = 400 \text{ m} ,$$

(Figure 3) and h_{in} (resp. h_{out}) is the water height at the inflow (resp. outflow).

In each case, the Manning's friction coefficient is $n = 0.03 \text{ m}^{-1/3}\text{s}$, the discharge q is taken equal to $20 \text{ m}^3\text{s}^{-1}$, the slope of the topography is given by:

$$S_0(x) = \left(1 - \frac{q^2(B(x) + 2Zh(x))}{g h(x)^3 (B(x) + Zh(x))^3} \right) h'(x) + q^2 n^2 \frac{(B(x) + 2h(x)\sqrt{1+Z^2})^{4/3}}{h(x)^{10/3} (B(x) + Zh(x))^{10/3}} - \frac{q^2 B'(x)}{g h(x)^2 (B(x) + Zh(x))^3}$$

where h is the water height and the topography is defined as $z(x) = \int_x^L S_0(X) dX$.

Remark 2 When programming these formulae, we noted a few typos in [35], in the expression of $S_0(x)$, of ϕ in the hydraulic jump case (§ 3.5.4) and in the formulation of h in $[0; 120]$ in the solution for the smooth transition followed by a hydraulic jump (§ 3.5.6).

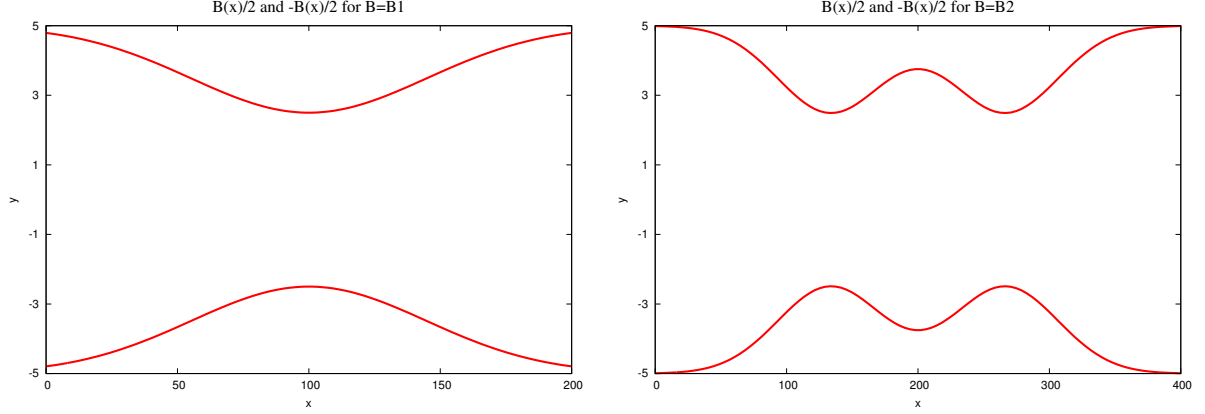


Figure 3: Functions B_1 and B_2 for the shape of the channel

Remark 3 We recall that the following analytic solutions are solutions of the pseudo-2D Shallow-Water system. This is the reason why, in this section, h_{ex} does not depend on y .

3.5.1 Subcritical flow in a short domain

In the case of a subcritical flow in a short domain, as in the three that follow, the cross section of the channel is rectangular, the bottom is given by the function B_1 and the length $L = 200$ m.

In this current case, the flow is fixed at inflow and the water height is prescribed at outflow. We have the following boundary conditions:

$$\begin{cases} \text{upstream: } q = 20 \text{ m}^3\text{s}^{-1}, \\ \text{downstream: } h = h_{out}. \end{cases}$$

The channel is initially dry, with a little puddle downstream, *i.e.* initial conditions are:

$$h(x, y) = \max(0, h_{out} + z(200, y) - z(x, y)) \text{ and } q = 0 \text{ m}^3/\text{s}.$$

If we take the mean water height

$$h_{ex}(x) = 0.9 + 0.3 \exp\left(-20 \left(\frac{x}{200} - \frac{1}{2}\right)^2\right),$$

the flow stays subcritical in the whole domain of length $L = 200$ m.

3.5.2 Supercritical flow in a short domain

In this case, the flow and the water height are fixed at inflow. We have the following boundary conditions:

$$\begin{cases} \text{upstream: } q = 20 \text{ m}^3\text{s}^{-1} \text{ and } h = h_{in}, \\ \text{downstream: free.} \end{cases}$$

The channel is initially dry, *i.e.* initial conditions are:

$$h = 0 \text{ m, and } q = 0 \text{ m}^3/\text{s}.$$

If we consider the mean water height

$$h_{ex}(x) = 0.5 + 0.5 \exp\left(-20 \left(\frac{x}{200} - \frac{1}{2}\right)^2\right),$$

in a channel of length $L = 200$ m with the B_1 shape and vertical boundary, the flow is supercritical.

3.5.3 Smooth transition in a short domain

In the case of smooth transition in a short domain, the flow is fixed at the inflow. We have the following boundary conditions:

$$\begin{cases} \text{upstream: } q = 20 \text{ m}^3\text{s}^{-1}, \\ \text{downstream: free.} \end{cases}$$

The channel is initially dry, *i.e.* initial conditions are:

$$h = 0 \text{ m, and } q = 0 \text{ m}^3/\text{s}.$$

The channel is the same as in the previous cases, with a mean water height given by

$$h_{ex}(x) = 1 - 0.3 \tanh\left(4\left(\frac{x}{200} - \frac{1}{3}\right)\right).$$

Under these conditions, the flow is first subcritical and becomes supercritical.

3.5.4 Hydraulic jump in a short domain

In the case of a hydraulic jump in a short domain, the flow discharge is fixed at the inflow and the water height is prescribed at both inflow and outflow. We have the following boundary conditions:

$$\begin{cases} \text{upstream: } q = 20 \text{ m}^3\text{s}^{-1} \text{ and } h = h_{in}, \\ \text{downstream: } h = h_{out}. \end{cases}$$

The channel is initially dry, with a little puddle downstream, *i.e.* initial conditions are:

$$h(x, y) = \max(0, h_{out} + z(200, y) - z(x, y)) \text{ and } q = 0 \text{ m}^3/\text{s}.$$

We choose the following expression for the mean water height:

$$h_{ex}(x) = 0.7 + 0.3 \left(\exp\left(\frac{x}{200}\right) - 1 \right) \quad \text{for } 0 \text{ m} \leq x \leq 120 \text{ m,}$$

and

$$h_{ex}(x) = \exp(-p(x - x^*)) \sum_{i=0}^M k_i \left(\frac{x - x^*}{x^{**} - x^*} \right)^i + \phi(x) \quad \text{for } 120 \text{ m} \leq x \leq 200 \text{ m,}$$

with:

- $x^* = 120 \text{ m,}$
- $x^{**} = 200 \text{ m,}$
- $M = 2,$
- $k_0 = -0.154375,$
- $k_1 = -0.108189,$
- $k_2 = -2.014310,$
- $p = 0.1,$
- $\phi(x) = 1.5 \exp\left(0.1\left(\frac{x}{200} - 1\right)\right).$

We obtain a supercritical flow that turns into a subcritical flow through a hydraulic jump.

3.5.5 Subcritical flow in a long domain

From now on, the length of the domain is $L = 400 \text{ m}$, the boundaries of the channel are given by B_2 and the cross sections are isoscele trapezoids.

In this case, the flow is fixed at the inflow and the water height is prescribed at the outflow. We have the following boundary conditions:

$$\begin{cases} \text{upstream: } q = 20 \text{ m}^3\text{s}^{-1}, \\ \text{downstream: } h = h_{out}. \end{cases}$$

The channel is initially dry, with a little puddle downstream, *i.e.* initial conditions are:

$$h(x, y) = \max(0, h_{out} + z(400, y) - z(x, y)) \text{ and } q = 0 \text{ m}^3/\text{s}.$$

Considering the mean water height

$$h_{ex}(x) = 0.9 + 0.3 \exp\left(-40 \left(\frac{x}{400} - \frac{1}{3}\right)^2\right) + 0.2 \exp\left(-35 \left(\frac{x}{400} - \frac{2}{3}\right)^2\right),$$

the flow is subcritical along the whole channel.

3.5.6 Smooth transition followed by a hydraulic jump in a long domain

In this case, the flow is fixed at the inflow and the water height is prescribed at the outflow. We have the following boundary conditions:

$$\begin{cases} \text{upstream: } q = 20 \text{ m}^3\text{s}^{-1}, \\ \text{downstream: } h = h_{out}. \end{cases}$$

The channel is initially dry, with a little puddle downstream, *i.e.* initial conditions are:

$$h(x, y) = \max(0, h_{out} + z(400, y) - z(x, y)) \text{ and } q = 0 \text{ m}^3/\text{s}.$$

With the second channel, we define the mean water height by

$$h_{ex}(x) = 0.9 + 0.25 \left(\exp\left(-\frac{x}{40}\right) - 1 \right) + 0.25 \exp\left(15 \left(\frac{x}{400} - \frac{3}{10}\right)\right) \quad \text{for } 0 \text{ m} \leq x \leq 120 \text{ m},$$

and

$$h_{ex}(x) = \exp(-p(x - x^*)) \sum_{i=0}^M k_i \left(\frac{x - x^*}{x^{**} - x^*}\right)^i + \phi(x) \quad \text{for } 120 \text{ m} \leq x \leq 200 \text{ m},$$

with:

- $x^* = 120 \text{ m}$,
- $x^{**} = 400 \text{ m}$,
- $M = 2$,
- $k_0 = -0.183691$,
- $k_1 = 1.519577$,
- $k_2 = -18.234429$,
- $p = 0.09$,
- $\phi(x) = 1.5 \exp\left(0.16 \left(\frac{x}{400} - 1\right)\right) - 0.3 \exp\left(2 \left(\frac{x}{400} - 1\right)\right)$.

Starting with a subcritical flow, we get a smooth transition to a supercritical zone, and, through a hydraulic jump, the flow becomes subcritical in the remaining of the domain.

4 Transitory solutions

In section 3, we gave steady-state solutions of increasing difficulties. These solutions can be used to check if the numerical methods are able to keep/catch steady-state flows. But even if the initial condition differs from the expected steady state, we do not have information about the transitory behavior. Thus, in this section, we list transitory solutions that may improve the validation of the numerical methods. Moreover, as most of these cases have wet/dry transitions, one can check the ability of the schemes to capture the evolution of these fronts (*e.g.* some methods may fail and give negative water height). At last, we give some periodic transitory solutions in order to check whether the schemes are numerically diffusive or not.

Table 3 lists all transitory solutions available in SWASHES and outlines their main features.

4.1 Dam breaks

In this section, we are interested in dam break solutions of increasing complexity on a flat topography namely Stoker's, Ritter's and Dressler's solutions. The analysis of dam break flow is part of dam design and safety analysis: dam breaks can release an enormous amount of water in a short time. This could be a threat to human life and to the infrastructures. To quantify the associated risk, a detailed description of

Transitory solutions				Slope			Friction				Comments
Type	Description	§	Reference	Null	Const.	Var.	Man.	D.-W.	Other	Null	
Dam breaks	Dam break on wet domain without friction	4.1.1	[46]	X						X	Moving shock. 1D
	Dam break on dry domain without friction	4.1.2	[42]	X						X	Wet-dry transition. 1D
	Dam break on dry domain with friction	4.1.3	[20]	X				X			Wet-dry transition. 1D
Oscillations without damping	Planar surface in a parabola	4.2.1	[48]			X				X	Wet-dry transition. 1D
	Radially-symmetrical paraboloid	4.2.2	[48]			X				X	Wet-dry transition. 2D
	Planar surface in a paraboloid	4.2.2	[48]			X				X	Wet-dry transition. 2D
Oscillations with damping	Planar surface in a parabola with friction	4.2.3	[43]			X			X		Wet-dry transition. 1D

Const.: Constant; Var.: Variable; Man.: Manning; D.-W.: Darcy-Weisbach

Table 3: Analytic solutions for shallow flow equations and their main features — Transitory cases

the dam break flood wave is required. Research on dam break started more than a century ago. In 1892, Ritter was the first who studied the problem, deriving an analytic solution based on the characteristics method (all the following solutions are generalizations of his method). He gave the solution for a dam break on a dry bed without friction (in particular, he considered an ideal fluid flow at the wavefront): it gives a parabolic water height profile connecting the upstream undisturbed region to the wet/dry transition point. In the 1950's, Dressler (see [20]) and Whitham (see [54]) derived analytic expressions for dam breaks on a dry bed including the effect of bed resistance with Chézy friction law. They both proved that the solution is equal to Ritter's solution behind the wave tip. But Dressler neglects the tip region (so his solution gives the location of the tip but not its shape) whereas Whitham's approach, by treating the tip thanks to an integral method, is more complete. Dressler compared these two solutions on experimental data [21]. A few years later, Stoker generalized Ritter's solution for a wet bed downstream the dam to avoid wet/dry transition.

Let us mention some other dam break solutions but we do not detail their expressions here. Ritter's solution has been generalized to a trapezoidal cross section channel thanks to Taylor's series in [55]. Dam break flows are also examined for problems in hydraulic or coastal engineering for example to discuss the behavior of a strong bore, caused by a tsunami, over a uniformly sloping beach. Thus in 1985 Matsutomi gave a solution of a dam break on a uniformly sloping bottom (as mentioned in [39]). Another contribution is the one of Chanson, who generalized Dressler's and Whitham's dam break solutions to turbulent and laminar flows with horizontal and sloping bottom [12, 13].

4.1.1 Dam break on a wet domain without friction

In the shallow water community, Stoker's solution or dam break on a wet domain is a classical case (introduced first in [46, p. 333–341]). This is a classical Riemann problem: its analog in compressible gas dynamics is the Sod tube [45] and in blood flow dynamics the ideal tourniquet [18]. In this section, we consider an ideal dam break on a wet domain, *i.e.* the dam break is instantaneous, the bottom is flat and there is no friction. We obtain an analytic solution of this case thanks to the characteristics method.

The initial condition for this configuration is the following Riemann problem

$$h(x) = \begin{cases} h_l & \text{for } 0 \leq x \leq x_0, \\ h_r & \text{for } x_0 < x \leq L, \end{cases}$$

with $h_l \geq h_r$ and $u(x) = 0$ m/s.

At time $t \geq 0$, we have a left-going rarefaction wave (or a part of parabola between $x_A(t)$ and $x_B(t)$) that reduces the initial depth h_l into h_m , and a right-going shock (located in $x_C(t)$) that increases the

initial height h_r into h_m . For each time $t \geq 0$, the analytic solution is given by

$$h(t, x) = \begin{cases} h_l & \\ \frac{4}{9g} \left(\sqrt{gh_l} - \frac{x - x_0}{2t} \right)^2 & \\ \frac{c_m^2}{g} & \\ h_r & \end{cases} \quad u(t, x) = \begin{cases} 0 \text{ m/s} & \text{if } x \leq x_A(t), \\ \frac{2}{3} \left(\frac{x - x_0}{t} + \sqrt{gh_l} \right) & \text{if } x_A(t) \leq x \leq x_B(t), \\ 2(\sqrt{gh_l} - c_m) & \text{if } x_B(t) \leq x \leq x_C(t), \\ 0 \text{ m/s} & \text{if } x_C(t) \leq x, \end{cases}$$

where

$$x_A(t) = x_0 - t\sqrt{gh_l}, \quad x_B(t) = x_0 + t(2\sqrt{gh_l} - 3c_m) \quad \text{and} \quad x_C(t) = x_0 + t\frac{2c_m^2(\sqrt{gh_l} - c_m)}{c_m^2 - gh_r},$$

with $c_m = \sqrt{gh_m}$ solution of $-8gh_r c_m^2 (\sqrt{gh_l} - c_m)^2 + (c_m^2 - gh_r)^2 (c_m^2 + gh_r) = 0$.

This solution tests whether the code gives the location of the moving shock properly.

In SWASHES, we take the following parameters for the dam: $h_l = 0.005$ m, $h_r = 0.001$ m, $x_0 = 5$ m, $L = 10$ m and $T = 6$ s.

4.1.2 Dam break on a dry domain without friction

Let us now look at Ritter's solution [42]: this is an ideal dam break (with a reservoir of constant height h_l) on a dry domain, *i.e.* as for the Stoker's solution, the dam break is instantaneous, the bottom is flat and there is no friction. The initial condition (Riemann problem) is modified and reads:

$$h(x) = \begin{cases} h_l > 0 & \text{for } 0 \text{ m} \leq x \leq x_0, \\ h_r = 0 \text{ m} & \text{for } x_0 < x \leq L, \end{cases}$$

and $u(x) = 0$ m/s. At time $t > 0$, the free surface is the constant water height (h_l) at rest connected to a dry zone (h_r) by a parabola. This parabola is limited upstream (resp. downstream) by the abscissa $x_A(t)$ (resp. $x_B(t)$). The analytic solution is given by

$$h(t, x) = \begin{cases} h_l & \\ \frac{4}{9g} \left(\sqrt{gh_l} - \frac{x - x_0}{2t} \right)^2 & \\ 0 \text{ m} & \end{cases} \quad u(t, x) = \begin{cases} 0 \text{ m/s} & \text{if } x \leq x_A(t), \\ \frac{2}{3} \left(\frac{x - x_0}{t} + \sqrt{gh_l} \right) & \text{if } x_A(t) \leq x \leq x_B(t), \\ 0 \text{ m/s} & \text{if } x_B(t) \leq x, \end{cases}$$

where

$$x_A(t) = x_0 - t\sqrt{gh_l} \quad \text{and} \quad x_B(t) = x_0 + 2t\sqrt{gh_l}.$$

This solution shows if the scheme is able to locate and treat correctly the wet/dry transition. It also emphasizes whether the scheme preserves the positivity of the water height, as this property is usually violated near the wetting front.

In SWASHES, we consider the numerical values: $h_l = 0.005$ m, $x_0 = 5$ m, $L = 10$ m and $T = 6$ s.

4.1.3 Dressler's dam break with friction

In this section, we consider a dam break on a dry domain with a friction term [20]. In the literature we may find several approaches for this case. Although it is not complete in the wave tip (behind the wet-dry transition), we present here Dressler's approach. Dressler considered Chézy friction law and used

a perturbation method in Ritter's method, *i.e.* u and h are expanded as power series in the friction coefficient $C_f = 1/C^2$.

The initial condition is

$$h(x) = \begin{cases} h_l > 0 & \text{for } 0 \text{ m} \leq x \leq x_0, \\ h_r = 0 \text{ m} & \text{for } x_0 < x \leq L, \end{cases}$$

and $u(x) = 0$ m/s. Dressler's first order developments for the flow resistance give the following corrected water height and velocity

$$\begin{cases} h_{co}(x, t) = \frac{1}{g} \left(\frac{2}{3} \sqrt{gh_l} - \frac{x - x_0}{3t} + \frac{g^2}{C^2} \alpha_1 t \right)^2, \\ u_{co}(x, t) = \frac{2\sqrt{gh_l}}{3} + \frac{2(x - x_0)}{3t} + \frac{g^2}{C^2} \alpha_2 t, \end{cases} \quad (16)$$

where

$$\alpha_1 = \frac{6}{5 \left(2 - \frac{x - x_0}{t\sqrt{gh_l}} \right)} - \frac{2}{3} + \frac{4\sqrt{3}}{135} \left(2 - \frac{x - x_0}{t\sqrt{gh_l}} \right)^{3/2}$$

and

$$\alpha_2 = \frac{12}{2 - \frac{x - x_0}{t\sqrt{gh_l}}} - \frac{8}{3} + \frac{8\sqrt{3}}{189} \left(2 - \frac{x - x_0}{t\sqrt{gh_l}} \right)^{3/2} - \frac{108}{7 \left(2 - \frac{x - x_0}{t\sqrt{gh_l}} \right)^2}.$$

With this approach, four regions are considered: from upstream to downstream, a steady state region ($(h_l, 0)$ for $x \leq x_A(t)$), a corrected region ((h_{co}, u_{co}) for $x_A(t) \leq x \leq x_T(t)$), the tip region (for $x_T(t) \leq x \leq x_B(t)$) and the dry region ($(0, 0)$ for $x_B(t) \leq x$). In the tip region, friction term is preponderant thus (16) is no more valid. In the corrected region, the velocity increases with x . Dressler assumed that at $x_T(t)$ the velocity reaches the maximum of u_{co} and that the velocity is constant in space in the tip region $u_{tip}(t) = \max_{x \in [x_A(t), x_B(t)]} u_{co}(x, t)$.

The analytic solution is then given by

$$h(t, x) = \begin{cases} h_l & \text{if } x \leq x_A(t), \\ h_{co}(x, t) & \text{if } x_A(t) \leq x \leq x_T(t), \\ h_{co}(x, t) & \text{if } x_T(t) \leq x \leq x_B(t), \\ 0 \text{ m} & \text{if } x_B(t) \leq x, \end{cases} \quad u(t, x) = \begin{cases} 0 \text{ m/s} & \text{if } x \leq x_A(t), \\ u_{co}(x, t) & \text{if } x_A(t) \leq x \leq x_T(t), \\ u_{tip}(t) & \text{if } x_T(t) \leq x \leq x_B(t), \\ 0 \text{ m/s} & \text{if } x_B(t) \leq x, \end{cases}$$

and with

$$x_A(t) = x_0 - t\sqrt{gh_l} \quad \text{and} \quad x_B(t) = x_0 + 2t\sqrt{gh_l}.$$

We should remark that with this approach the water height is not modified in the tip zone. This is a limit of Dressler's approach. Thus we coded the second order interpolation used in [50, 51] (not detailed here) and recommended by Valerio Caleffi¹.

Even if we have no information concerning the shape of the wave tip, this case shows if the scheme is able to locate and treat correctly the wet/dry transition.

In SWASHES, we have $h_l = 6$ m, $x_0 = 1000$ m, $C = 40$ m^{1/2}/s (Chezy coefficient), $L = 2000$ m and $T = 40$ s.

¹Personal communication

4.2 Oscillations

In this section, we are interested in Thacker's and Sampson's solutions. These are analytic solutions with a variable slope (in space) for which the wet/dry transitions are moving. Such moving-boundary solutions are of great interest in communities interested in tsunami run-up and ocean flow simulations (see among others [37], [33] and [41]). A prime motivation for these solutions is to provide tests for numerical techniques and codes in wet/dry transitions on varying topographies. The first moving-boundary solutions of Shallow-Water equations for a water wave climbing a linearly sloping beach is obtained in [11] (thanks to a hodograph transformation). Using Shallow-Water equations in Lagrangian form, Miles and Ball [40] and [3] mentioned exact moving-boundary solutions in a parabolic trough and in a paraboloid of revolution. In [48], Thacker shows exact moving boundary solutions using Eulerian equations. His approach was first to make assumptions about the nature of the motion and then to solve the basin shape in which that motion is possible. His solutions are analytic periodic solutions (there is no damping) with Coriolis effect. Some of these solutions were generalised by Sampson *et al.* [43, 44] by adding damping due to a linear friction term.

Thacker's solutions described here do not take into account Coriolis effect. In the 1D case, the topography is a parabola and in the 2D case it is a paraboloid. These solutions test the ability of schemes to simulate flows with comings and goings and, as the water height is periodic in time, the numerical diffusion of the scheme. Similarly to the dam breaks on a dry domain, Thacker's solutions also test wet/dry transition.

4.2.1 Planar surface in a parabola without friction

Each solution written by Thacker has two dimensions in space [48]. The exact solution described here is a simplification to 1D of an artificially 2D Thacker's solution. Indeed, for this solution, Thacker considered an infinite channel with a parabolic cross section but the velocity has only one nonzero component (orthogonal to the axis of the channel). This case provides us with a relevant test in 1D for shallow water model because it deals with a sloping bed as well as with wetting and drying. The topography is a parabolic bowl given by

$$z(x) = h_0 \left(\frac{1}{a^2} \left(x - \frac{L}{2} \right)^2 - 1 \right),$$

and the initial condition on the water height is

$$h(x) = \begin{cases} -h_0 \left(\left(\frac{1}{a} \left(x - \frac{L}{2} \right) + \frac{B}{\sqrt{2gh_0}} \right)^2 - 1 \right) & \text{for } x_1(0) \leq x \leq x_2(0), \\ 0 \text{ m} & \text{otherwise,} \end{cases}$$

with $B = \sqrt{2gh_0}/(2a)$ and for the velocity $u(x) = 0$ m/s. Thacker's solution is a periodic solution (without friction) and the free surface remains planar in time. The analytic solution is

$$h(t, x) = \begin{cases} -h_0 \left(\left(\frac{1}{a} \left(x - \frac{L}{2} \right) + \frac{B}{\sqrt{2gh_0}} \cos \left(\frac{\sqrt{2gh_0}}{a} t \right) \right)^2 - 1 \right) & \text{for } x_1(t) \leq x \leq x_2(t), \\ 0 \text{ m} & \text{otherwise,} \end{cases}$$

$$u(t, x) = \begin{cases} B \sin \left(\frac{\sqrt{2gh_0}}{a} t \right) & \text{for } x_1(t) \leq x \leq x_2(t), \\ 0 \text{ m/s} & \text{otherwise.} \end{cases}$$

where $x_1(t)$ and $x_2(t)$ are the locations of wet/dry interfaces at time t

$$x_1(t) = -\frac{1}{2} \cos\left(\frac{\sqrt{2gh_0}}{a}t\right) - a + \frac{L}{2},$$

$$x_2(t) = -\frac{1}{2} \cos\left(\frac{\sqrt{2gh_0}}{a}t\right) + a + \frac{L}{2}.$$

In SWASHES, we consider $a = 1$ m, $h_0 = 0.5$ m, $L = 4$ m and $T = 10.0303$ s (5 periods).

4.2.2 Two dimensional cases

Several two dimensional exact solutions with moving boundaries were developed by Thacker. Most of them include the Coriolis force that we do not consider here (for further information, see [48]). These solutions are periodic in time with moving wet/dry transitions. They provide perfect tests for shallow water as they deal with bed slope and wetting/drying with two dimensional effects. Moreover, as the solution is exact without discontinuity, it is very appropriate to verify the accuracy of a numerical method.

Radially-symmetrical paraboloid The two dimensional case presented here is a radially symmetrical oscillating paraboloid [48]. The solution is periodic without damping (*i.e.* no friction). The topography is a paraboloid of revolution defined by

$$z(r) = -h_0 \left(1 - \frac{r^2}{a^2}\right) \quad (17)$$

with $r = \sqrt{(x - L/2)^2 + (y - L/2)^2}$ for each (x, y) in $[0; L] \times [0; L]$, where h_0 is the water depth at the central point of the domain for a zero elevation and a is the distance from this central point to the zero elevation of the shoreline. The solution is given by:

$$\begin{cases} h(r, t) = h_0 \left(\frac{\sqrt{1-A^2}}{1-A\cos(\omega t)} - 1 - \frac{r^2}{a^2} \left(\frac{1-A^2}{(1-A\cos(\omega t))^2} - 1 \right) \right) - z(r) \\ u(x, y, t) = \frac{1}{1-A\cos(\omega t)} \left(\frac{1}{2}\omega \left(x - \frac{L}{2} \right) A \sin(\omega t) \right) \\ v(x, y, t) = \frac{1}{1-A\cos(\omega t)} \left(\frac{1}{2}\omega \left(y - \frac{L}{2} \right) A \sin(\omega t) \right) \end{cases}$$

where the frequency ω is defined as $\omega = \sqrt{8gh_0}/a$, r_0 is the distance from the central point to the point where the shoreline is initially located and $A = (a^2 - r_0^2)/(a^2 + r_0^2)$ (Figure 4).

The analytic solution at $t = 0$ s is taken as initial condition.

In SWASHES, we consider $a = 1$ m, $r_0 = 0.8$ m, $h_0 = 0.1$ m, $L = 4$ m and $T = 3\frac{2\pi}{\omega}$.

Planar surface in a paraboloid For this second Thacker's 2D case, the moving shoreline is a circle and the topography is again given by (17). The free surface has a periodic motion and remains planar in time [48]. To visualize this case, one can think of a glass with some liquid in rotation inside.

The exact periodic solution is given by:

$$\begin{cases} h(x, y, t) = \frac{\eta h_0}{a^2} \left(2 \left(x - \frac{L}{2} \right) \cos(\omega t) + 2 \left(y - \frac{L}{2} \right) \sin(\omega t) - \eta \right) - z(x, y) \\ u(x, y, t) = -\eta\omega \sin(\omega t) \\ v(x, y, t) = \eta\omega \cos(\omega t) \end{cases}$$

for each (x, y) in $[0; L] \times [0; L]$, where the frequency ω is defined as $\omega = \sqrt{2gh_0}/a$ and η is a parameter. Here again, the analytic solution at $t = 0$ s is taken as initial condition.

In SWASHES, we consider $a = 1$ m, $h_0 = 0.1$ m, $\eta = 0.5$, $L = 4$ m and $T = 3\frac{2\pi}{\omega}$.

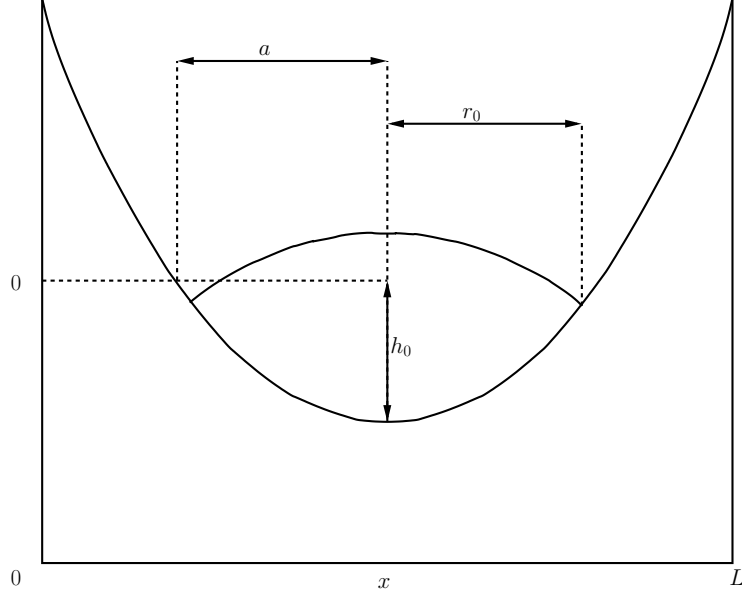


Figure 4: Notations for Thacker's axisymmetrical solution

4.2.3 Planar surface in a parabola with friction

Considering a linear friction term (*i.e.* $S_f = \tau u/g$) in system (2) (with $R = 0$ m/s and $\mu = 0$ m²/s) with Thacker's approach, Sampson *et al.* got moving boundaries solutions with damping [43, 44]. These solutions provide a set of 1D benchmarks for numerical techniques in wet/dry transitions on varying topographies (as Thacker's solutions) and with a friction term. One of these solutions is presented here. The topography is a parabolic bowl given by

$$z(x) = h_0 \frac{\left(x - \frac{L}{2}\right)^2}{a^2},$$

where h_0 and a are two parameters and $x \in [0, L]$. The initial free surface is

$$(z + h)(x) = \begin{cases} h_0 + \frac{a^2 B^2}{8g^2 h_0} \left(\frac{\tau^2}{4} - s^2\right) - \frac{B^2}{4g} - \frac{1}{g} B s \left(x - \frac{L}{2}\right) & \text{for } x_1(0) \leq x \leq x_2(0), \\ 0 \text{ m} & \text{else,} \end{cases}$$

with B a constant, $s = \sqrt{p^2 - \tau^2}/2$ and $p = \sqrt{8gh_0/a^2}$. The free surface remains planar in time

$$(z + h)(t, x) = \begin{cases} h_0 + \frac{a^2 B^2 e^{-\tau t}}{8g^2 h_0} \left(-s\tau \sin(2st) + \left(\frac{\tau^2}{4} - s^2\right) \cos(2st)\right) \\ - \frac{B^2 e^{-\tau t}}{4g} - \frac{e^{-\tau t/2}}{g} \left(Bs \cos(st) + \frac{\tau B}{2} \sin(st)\right) \left(x - \frac{L}{2}\right) & \text{for } x_1(t) \leq x \leq x_2(t), \\ z(x) & \text{else} \end{cases}$$

and the velocity is given by

$$u(t, x) = \begin{cases} B e^{-\tau t/2} \sin(st) & \text{for } x_1(t) \leq x \leq x_2(t), \\ 0 \text{ m/s} & \text{else.} \end{cases}$$

The wet/dry transitions are located at $x_1(t)$ and $x_2(t)$

$$x_1(t) = \frac{a^2 e^{-\tau t/2}}{2gh_0} \left(-Bs \cos(st) - \frac{\tau B}{2} \sin(st) \right) - a + \frac{L}{2},$$

$$x_2(t) = \frac{a^2 e^{-\tau t/2}}{2gh_0} \left(-Bs \cos(st) - \frac{\tau B}{2} \sin(st) \right) + a + \frac{L}{2}.$$

In SWASHES, we consider $a = 3,000$ m, $h_0 = 10$ m, $\tau = 0.001$ s⁻¹, $B = 5$ m/s, $L = 10,000$ m and $T = 6,000$ s.

5 The SWASHES software

In this section, we describe the Shallow Water Analytic Solutions for Hydraulic and Environmental Studies (SWASHES) software. At the moment, SWASHES includes all the analytic solutions given in this paper. The source code is freely available to the community through the SWASHES repository hosted at <http://www.univ-orleans.fr/mapmo/soft/SWASHES>. It is distributed under CeCILL-V2 (GPL-compatible) free software license.

When running the program, the user must specify in the command line the choice of the solution (namely the dimension, the type, the domain and the number of the solution) as well as the number of cells for the discretization of the analytic solution. The solution is computed and can be redirected in a gnuplot-compatible ASCII file.

SWASHES is written in object-oriented ISO C++. The program is structured as follows: each type of solutions, such as *bump*, *dam_break*, *Thacker*, etc., is written in a specific class. This structure gives the opportunity to easily implement a new solution, whether in a class that already exists (for example a new Mac Donald type solution), or in a new class. Each analytic solution is coded with specific parameters (most of them taken from [16]). In fact, all the parameters are written in the code, except the number of cells.

We claim that such a library can be useful for developers of Shallow-Water codes to evaluate the performances and properties of their own code, each analytic solution being a potential piece of benchmark. Depending on the targeted applications and considering the wide range of flow conditions available among the analytic solutions, developers may select a subset of the analytic solutions available in SWASHES. We recommend not to change the values of the parameters to ease the comparison of numerical methods among different codes. However, it may be legitimate to modify these parameters to adapt the case to other specific requirements (friction coefficient, dam break height, rain intensity, etc.). This can be easily done in SWASHES but, in that case, the code must be renamed to avoid confusions.

6 Some numerical results: comparison with FullSWOF approximate solutions

SWASHES was created because we have been developing a software for the resolution of Shallow-Water equations, namely FullSWOF, and we wanted to validate it against analytic solutions. To illustrate the use of SWASHES in a practical case, we first give a short description of the 1D and 2D codes of FullSWOF and then we compare the results of FullSWOF with the analytic solutions. The comparisons between FullSWOF results and the analytic solutions is based on the relative error in percentage of the water height, using, of course, the analytic solution as a reference. This percentage is positive when FullSWOF overestimates the water height and negative when it underestimates it.

6.1 The FullSWOF program

FullSWOF (Full Shallow-Water equations for Overland Flow) is an object-oriented C++ code (free software and GPL-compatible license CeCILL-V2². Source code available at <http://www.univ-orleans.fr/mapmo/soft/FullSWOF/>) developed in the framework of the multidisciplinary project METHODE (see [15, 16] and <http://www.univ-orleans.fr/mapmo/methode/>). We briefly describe here the principles of the numerical methods used in FullSWOF_2D. The main strategy consists in a finite volume method on a structured mesh in two space dimensions. Structured meshes have been chosen because on the one hand digital topographic maps are often provided on such grids, and, on the other hand, it allows to develop numerical schemes in one space dimension (implemented in FullSWOF_1D), the extension to dimension two being then straightforward. Finite volume method ensures by construction the conservation of the water mass, and is coupled with the hydrostatic reconstruction [2, 7] to deal with the topography source term. This reconstruction preserves the positivity of the water height and provides a well-balanced scheme (notion introduced in [28]) *i.e.* it preserves at least hydrostatic equilibrium (9) (typically puddles and lakes). Several numerical fluxes and second order reconstructions are implemented. Currently, we recommend, based on [16], to use the second order scheme with MUSCL reconstruction [52] and HLL flux [29]. FullSWOF is structured in order to ease the implementation of new numerical methods.

6.2 Examples in one dimension

In this part, we give the results obtained with FullSWOF_1D for three one-dimensional cases. For these examples, we have 500 cells on the FullSWOF_1D domain but 2500 for semi-analytic solutions (see Remark 1). In some figures, we also plotted the critical height, in order to show directly whether the flow is fluvial or torrential.

6.2.1 Bumps

Lake at rest with an immersed bump On Figure 5, we plotted the solution and the water flow for a lake at rest with an immersed bump (Section 3.1.1) for a large time, namely $t = 100$ s.

First, the water height seems to stay constant as expected. On the second figure, we see that the numerical approximations of FullSWOF_1D return a water flow of order 10^{-7} m²/s instead of zero, which is quite good.

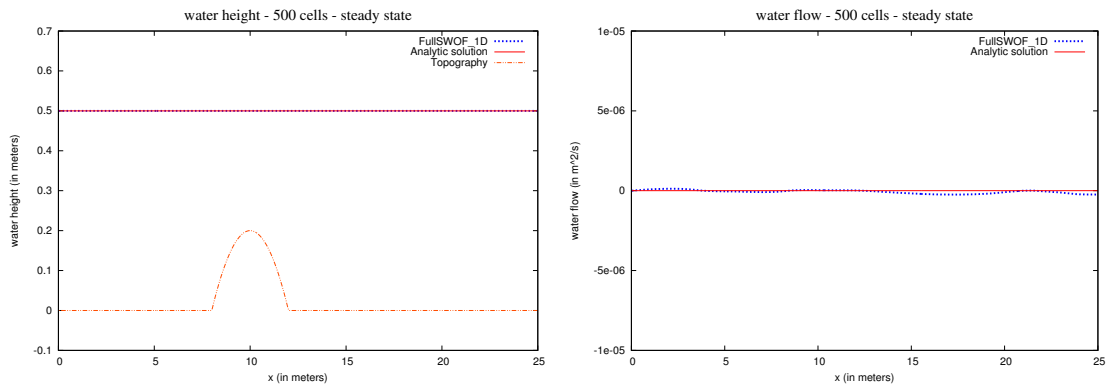


Figure 5: Results of FullSWOF_1D for a lake at rest with an immersed bump

²<http://www.cecill.info/index.en.html>

Lake at rest with an emerged bump As in the previous case, on Figure 6, we plotted the solution and the water flow for a lake at rest, but with an emerged bump (and consequently with wet / dry transitions, see Section 3.1.2), with $t = 100$ s.

Again, we note that the water height is not modified by FullSWOF_1D as expected and the water flow is of order 10^{-9} m²/s instead of zero.

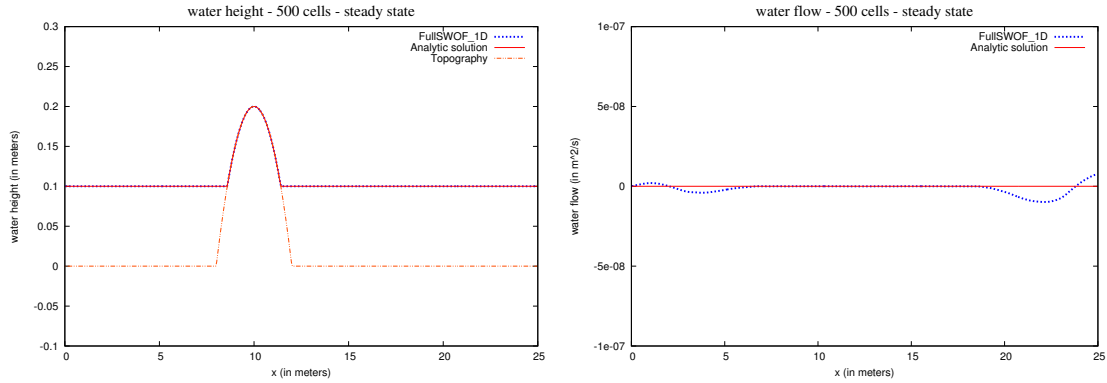


Figure 6: Results of FullSWOF_1D for a lake at rest with an emerged bump

Subcritical flow On Figure 7, we can see the results in the case of a subcritical flow over a bump (see Section 3.1.3), at the steady state ($t = 100$ s).

The water height is larger than the critical height, then the flow is subcritical. The approximated solution follows the analytic solution of SWASHES.

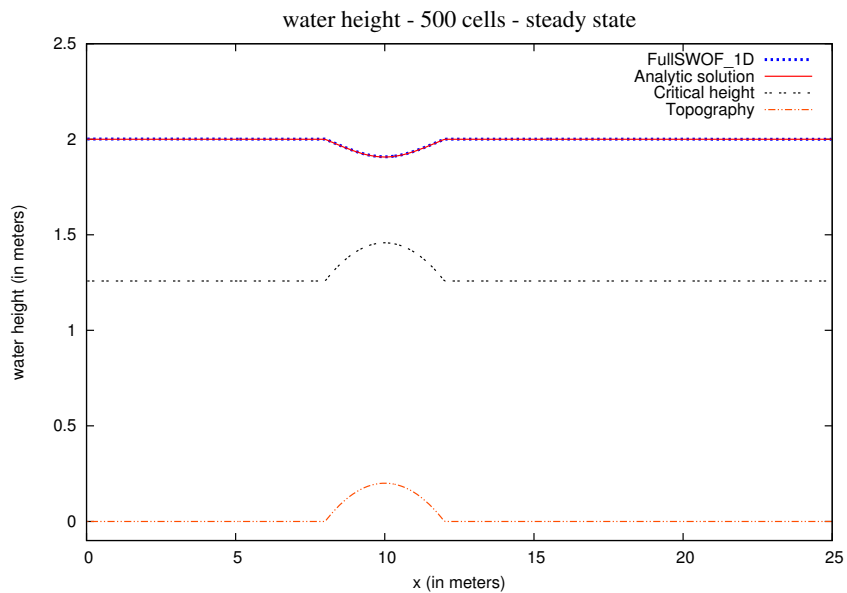


Figure 7: Results of FullSWOF_1D for a subcritical flow

Transcritical flow without shock We plotted the results obtained for the transcritical flow without shock (see Section 3.1.4) on Figure 8, with $t = 100$ s.

We can see that the solution is well caught by FullSWOF_1D, and that the flow is subcritical on the left part of the bump, supercritical on the right part of the bump.

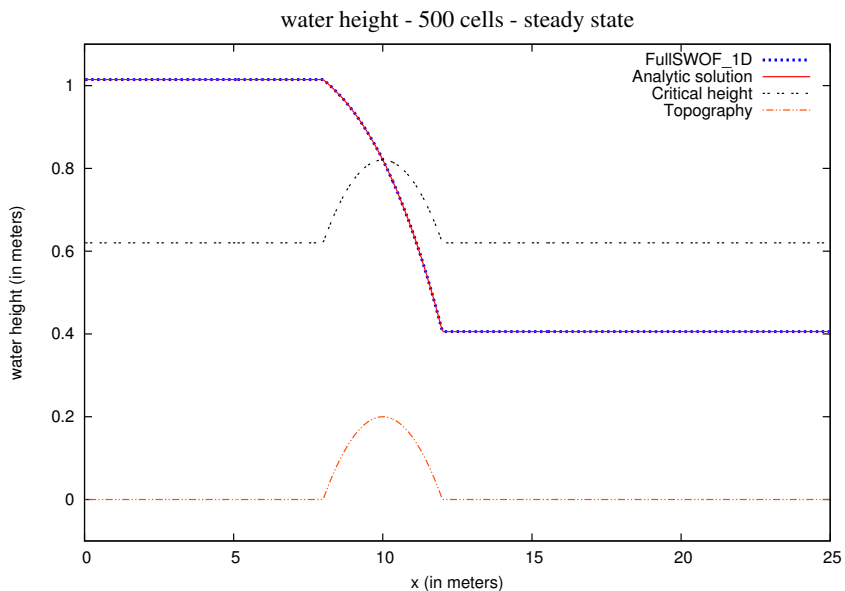


Figure 8: Results of FullSWOF_1D for a transcritical flow without shock

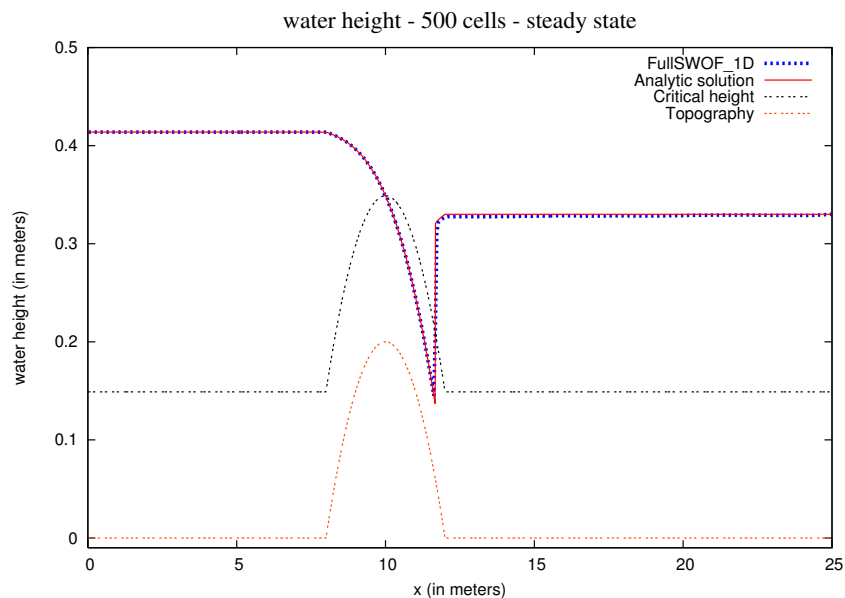


Figure 9: Results of FullSWOF_1D for a transcritical flow with shock

Transcritical flow with shock On Figure 9, we plotted the solution for a transcritical flow with shock (Section 3.1.5) for a time large enough to attain the steady state, namely $t = 100$ s.

Overall, the numerical result of FullSWOF_1D and the analytic solution are in very good agreement. By looking carefully at the differences in water height, it appears that the difference is extremely low before the bump (-4×10^{-6} m, *i.e.* -0.001%). Right at the beginning of the bump, this difference increases to +0.06%, but on a single cell. Over the bump, differences are alternatively positive and negative which leads, overall, to a good estimate. A maximum (+1.2%) is reached exactly at the top of the bump (*i.e.* at the transition from subcritical flow to supercritical flow). Just before the shock, the difference is only +0.03%. The largest difference in height (+100%) is achieved at the shock and affects a single cell. While for the analytic solution the shock is extremely sharp, in FullSWOF_1D it spans over four cells. After the shock and up to the outlet, the heights computed by FullSWOF_1D remain lower than the heights of the analytic solution, going from -1% (after the shock) to -0.01% (at the outflow boundary condition).

6.2.2 Mac Donald's type 1D solutions – long channel: 1000 m

Let us study the solutions of the Mac Donald's type in one dimension, for a long channel, see Section 3.2.1. We recall that the analytic solution is computed with a lot of cell points (we choose 5000 points) to be sure to be precise enough, see remark 1.

Subcritical case We consider the results of the subcritical case on Figure 10, with $t = 1500$ s and for both Darcy-Weisbach's and Manning's friction laws.

First, one can note that the difference in the friction terms does not give the same topography, due to the formula 11. But in both cases, the fluvial steady state is obtained by FullSWOF_1D.

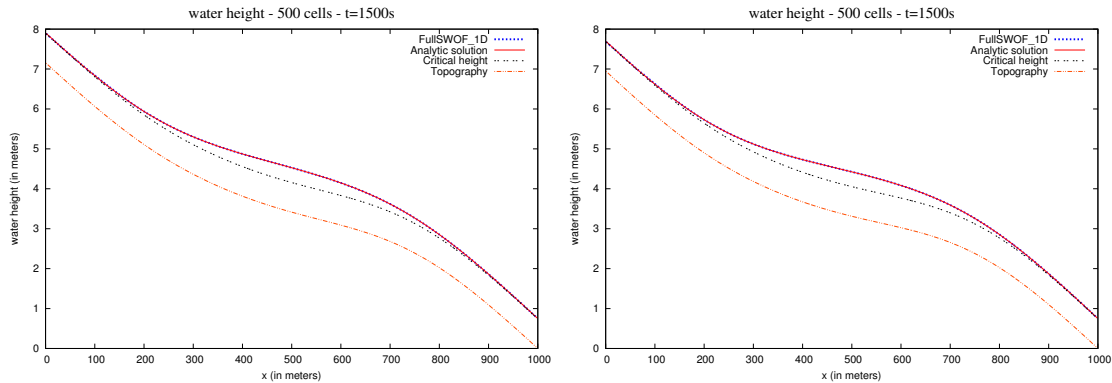


Figure 10: Results of FullSWOF_1D for a long channel with a subcritical flow; Darcy-Weisbach's friction law on the left, Manning's friction law on the right

Supercritical case Let us turn to the supercritical case, see Figure 11.

The analytic solution and the solution computed by FullSWOF_1D are the same, slightly below the critical height.

Subcritical-to-supercritical case On Figure 12, we plotted the results for the subcritical to supercritical case.

This transcritical case does not bring any difficulty to FullSWOF_1D, as it follows the analytic solution of SWASHES.

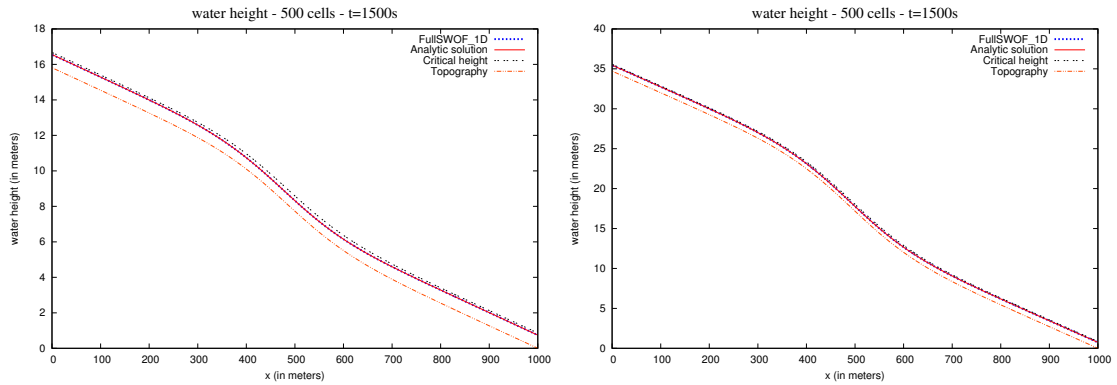


Figure 11: Results of FullSWOF_1D for a long channel with a supercritical flow; Darcy-Weisbach's friction law on the left, Manning's friction law on the right

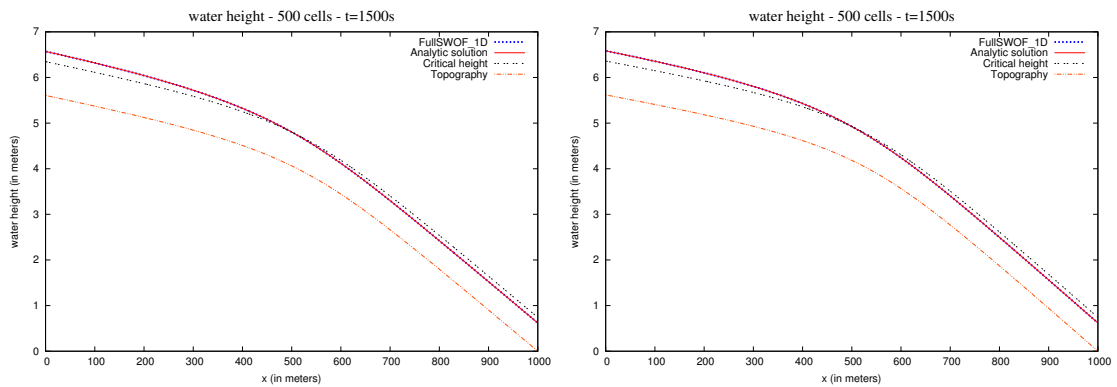


Figure 12: Results of FullSWOF_1D for a long channel with a subcritical-to-supercritical flow; Darcy-Weisbach's friction law on the left, Manning's friction law on the right

Supercritical-to-subcritical case Last case for this long channel, we give the results for the supercritical to subcritical case, with a shock, see Figure 13.

The shock located at the center of the domain is well caught by FullSWOF_1D.

6.2.3 Mac Donald's type 1D solutions – short channel: 100 m

The three solutions of this section correspond to the short channel, see Section 3.2.2

Smooth transition and shock in a short domain Figure 14 shows the case of a smooth transition and a shock in a short domain (Section 3.2.2). The final time is $t = 150$ s.

FullSWOF_1D result is very close to the analytic solution. From $x = 0$ m to the subcritical-to-supercritical transition, FullSWOF_1D underestimates slightly the water height and the difference grows smoothly with x (to -0.1%). Around $x = 45$ m (*i.e.* close to the subcritical-to-supercritical transition), the difference remains negative but oscillates, reaching a maximum difference of -0.22%. After this transition, FullSWOF_1D continues to underestimate the water height and this difference grows smoothly up to -0.5% right before the shock. As for the comparison with the transcritical flow with shock (see Section 6.2.1), the maximum difference is reached exactly at the shock ($x = 66.6$ m): FullSWOF_1D overestimates

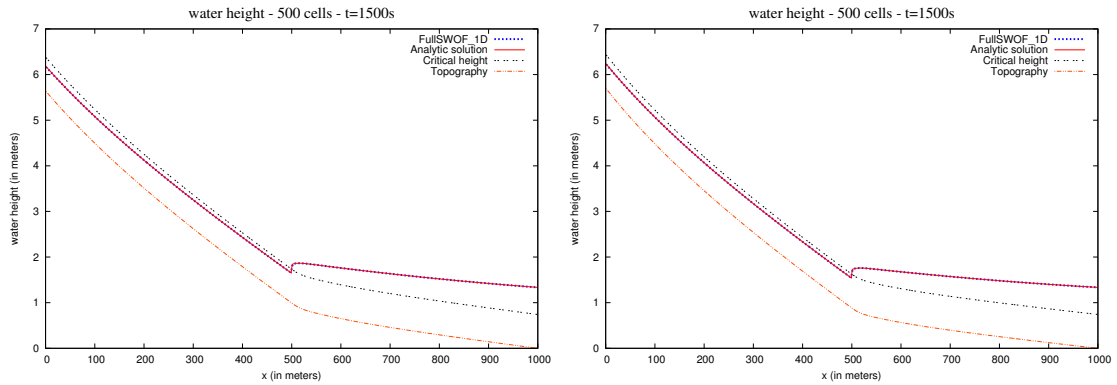


Figure 13: Results of FullSWOF_1D for a long channel with a supercritical-to-subcritical flow; Darcy-Weisbach's friction law on the left, Manning's friction law on the right

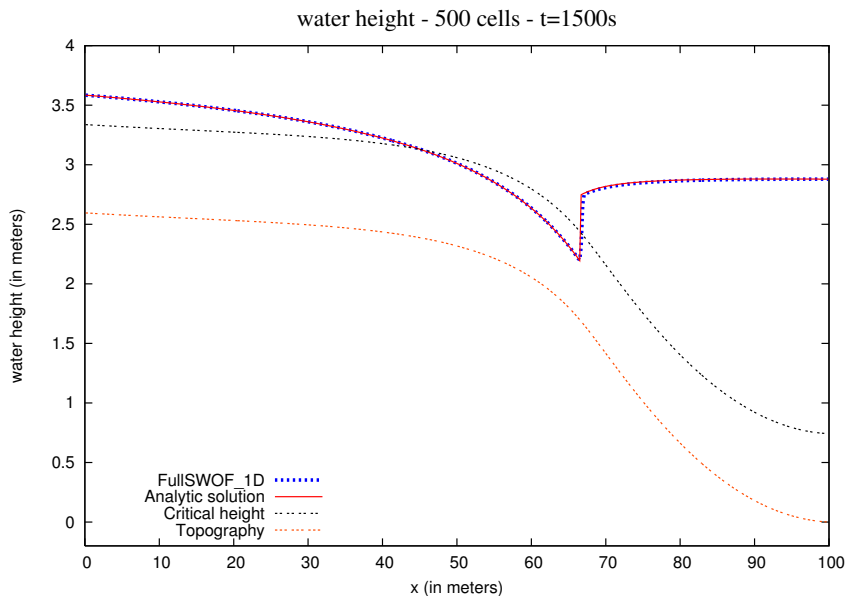


Figure 14: Results of FullSWOF_1D for the Mac Donald's type solution with a smooth transition and a shock in a short domain, with Manning's friction coefficient

water height by +24%. Right after the shock, the overestimation is only +1% and decreases continuously downstream, reaching 0% at the outlet.

Supercritical case The results for the supercritical case are plotted on Figure 15.

The flow is supercritical (below the critical height) and the numerical solution is well computed.

Subcritical-to-supercritical case On the last figure of this section, Figure 16, we give the subcritical to supercritical solution for the Mac Donald's type problem in one dimension.

Note that, due to the initial condition, to get this result with the appropriate regimes, it is necessary to impose in FullSWOF_1D a water height bigger than the critical height on the left boundary and smaller

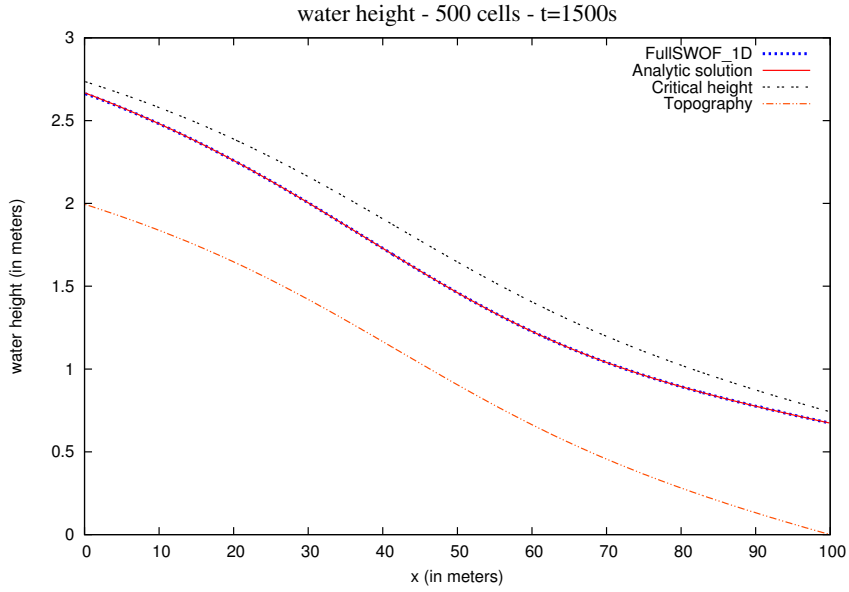


Figure 15: Results of FullSWOF_1D for the supercritical Mac Donald's type solution in a short domain, with Manning's friction coefficient

than the critical height on the right boundary (with $h_c \approx 0.74$ m). With this parametrization, we obtain a good approximation of the analytic solution, starting in a subcritical flow and becoming supercritical on the right part of the domain.

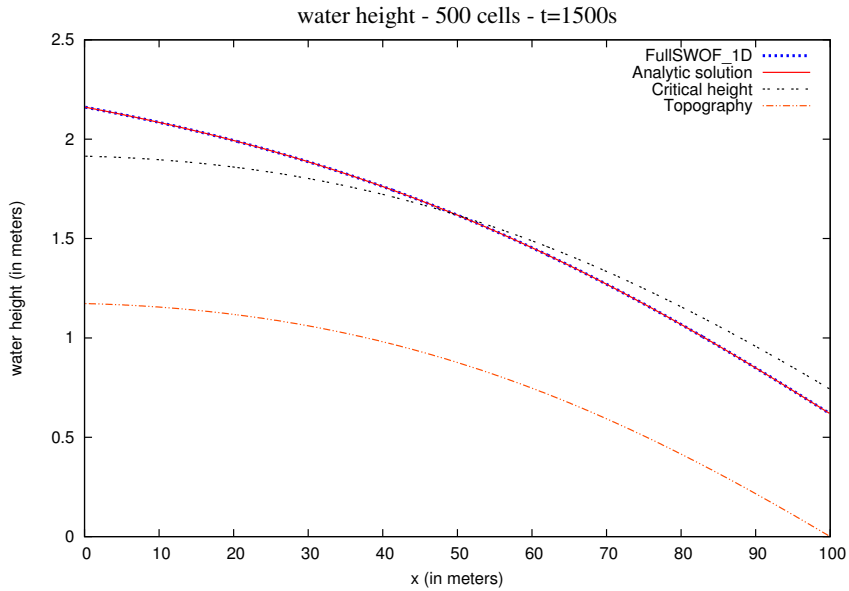


Figure 16: Results of FullSWOF_1D for the supercritical to subcritical Mac Donald's type solution in a short domain, with Manning's friction coefficient

6.2.4 Mac Donald's type 1D solutions – long channel: 5000 m, periodic and subcritical

In this section, we are interested in the results of the very long channel, with an oscillating topography, in a subcritical case, see Section 3.2.3. As the channel is very long, we have to take a long time to be at the steady state, namely $t = 3000$ s, and we get the results on Figure 17.

We can notice that the oscillating solution is obtained by FullSWOF_1D. The water starts to spread from the left, until the periodic steady state is reached.

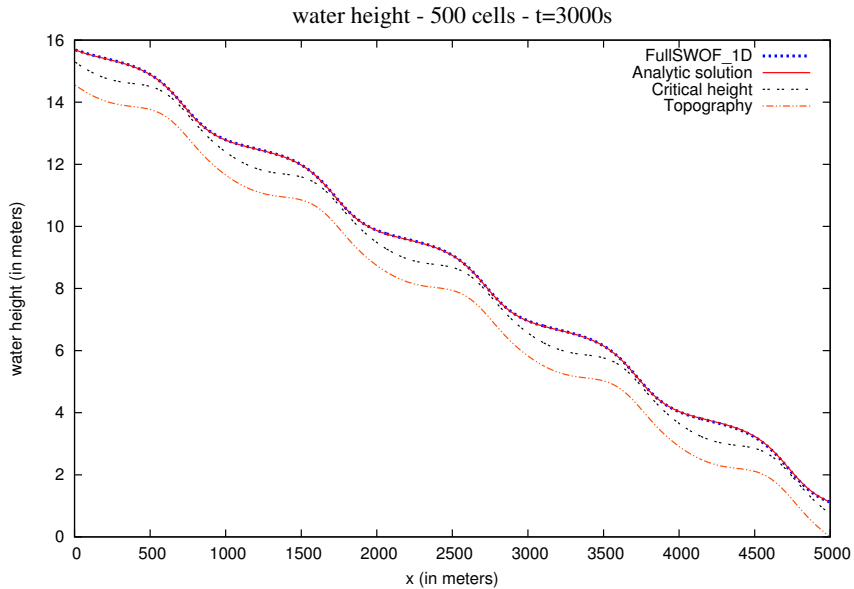


Figure 17: Results of FullSWOF_1D for the Mac Donald's type solution with a very long channel and oscillating topography, in a subcritical case, with Manning's friction coefficient

6.2.5 Mac Donald's type 1D solutions with rain

In this section, we consider Mac Donald's type solutions with rain, see Section 3.3

Subcritical case for a long channel The first case is a subcritical case, see Section 3.3.1. As the rain is started at $t = 1500$ s, we let the simulation until $t = 3000$ s, see Figure 18

As in the previous examples, the numerical results given by FullSWOF_1D are a very good approximation of the analytic solution: this is a way to validate the implementation of the rain term.

Supercritical case for a long channel Then, on Figure 19, we plotted the case of a supercritical flow, see Section 3.3.2

Even for the supercritical regime, the analytic solution is well approximated and the rain does not bring any spurious behavior.

6.2.6 Mac Donald's type 1D solutions with diffusion

This section is devoted to the Mac Donald's type 1D solutions with diffusion, see Section 3.4. However, the diffusion is not available in FullSWOF yet. So, in the next two figures, we only give the analytic results.

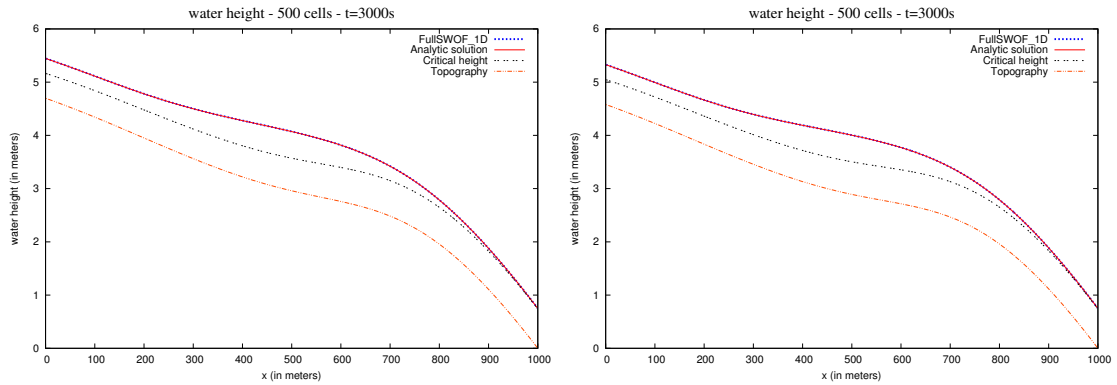


Figure 18: Results of FullSWOF_1D for a long channel with a subcritical flow; Darcy-Weisbach's friction law on the left, Manning's friction law on the right

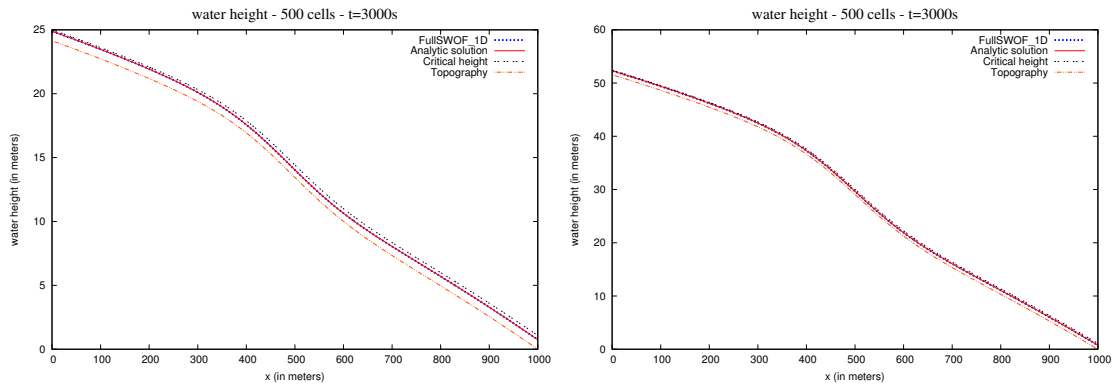


Figure 19: Results of FullSWOF_1D for a long channel with a supercritical flow; Darcy-Weisbach's friction law on the left, Manning's friction law on the right

Subcritical case for a long channel On Figure 20, we give the analytic solution for the subcritical case detailed in Section 3.4.1.

Supercritical case for a long channel For the supercritical case, the analytic solution is explained in Section 3.4.2 and the curves are depicted on Figure 21.

6.2.7 Dam breaks

Dam break on a wet domain For the first dam break case, we consider a dam break on a wet domain, see Section 4.1.1. The results are plotted in Figure 22 at time $t = 6$ s.

FullSWOF_1D gives the same values as the analytic solution on the three plateaus, but the curve is a little bit smoothed where the analytic solution shows sharp angles.

Dam break on a dry domain The last figure for the one-dimensional case is Figure 23, with the solution of a dam break on a dry domain (Section 4.1.2). We chose the final time equal to $t = 6$ s. Here too, the numerical result of FullSWOF_1D matches with the analytic solution well. The height differences on the plateau ($h = 0.005$ m) are null. On this domain, the water is not flowing yet. This

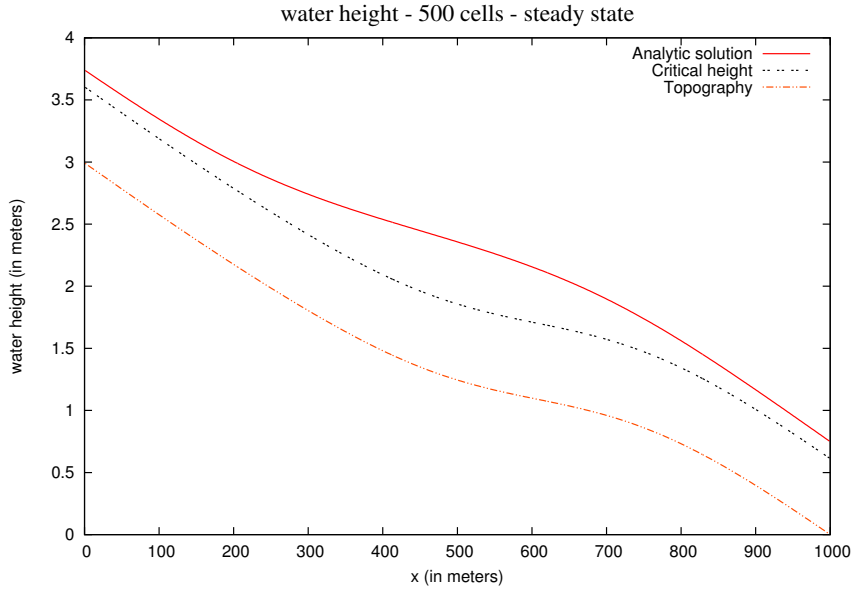


Figure 20: Analytic solution for the subcritical Mac Donald's type solution with diffusion

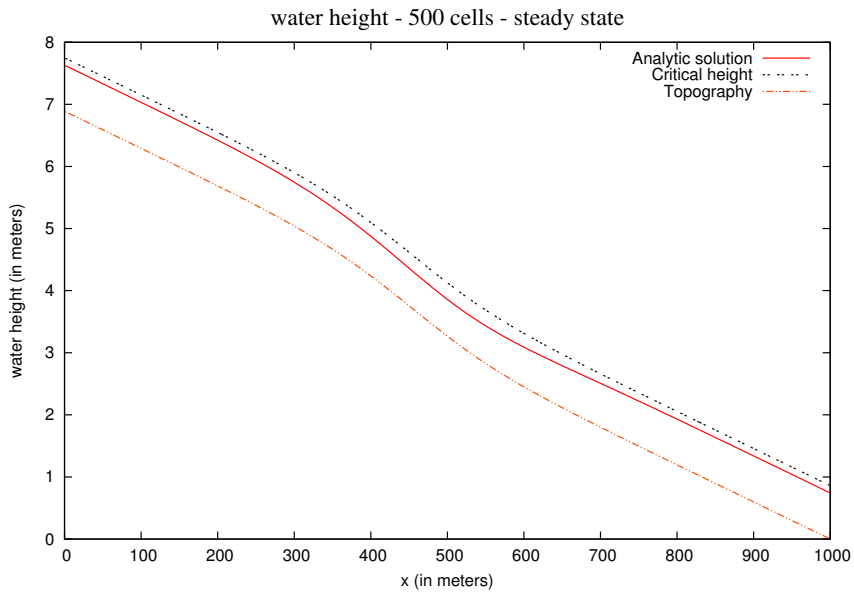


Figure 21: Analytic solution for the supercritical Mac Donald's type solution with diffusion

shows FullSWOF_1D preserves steady-states at rest properly. The analytic solution predicts a kink at $x = 3.7$ m. In FullSWOF_1D result, it does not show a sharp angle but a curve: FullSWOF_1D slightly underestimates the water height (by a maximum of -2%) between $x = 3.4$ m and $x = 4$ m. Between $x = 4$ m and $x = 6.9$ m, FullSWOF_1D overestimates constantly the water height (by up to +2%). On all the domain between $x = 6.9$ m and $x = 7.6$ m, the water height predicted by FullSWOF_1D is lower than the water height computed by the analytic solution (by as much as -100%). At this water front,

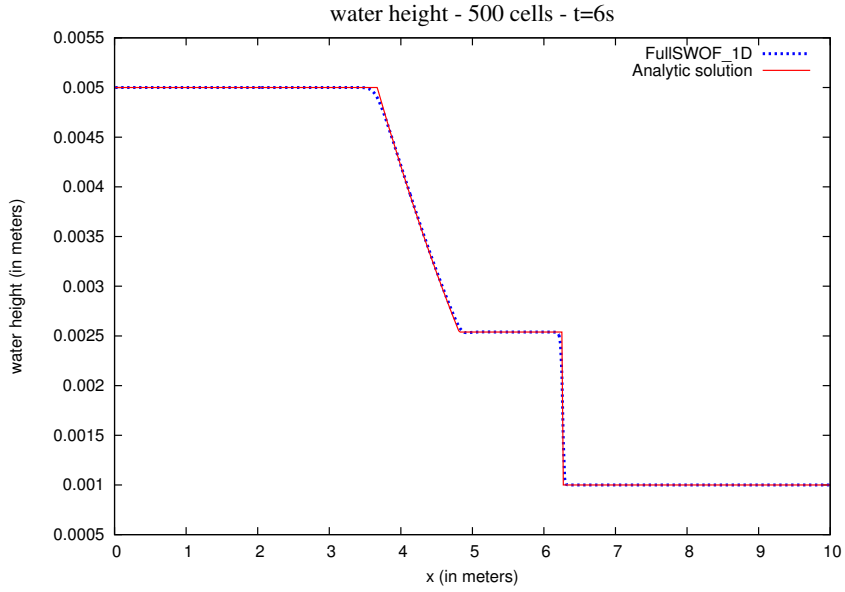


Figure 22: Results of FullSWOF_1D for a dam break on a wet domain without friction

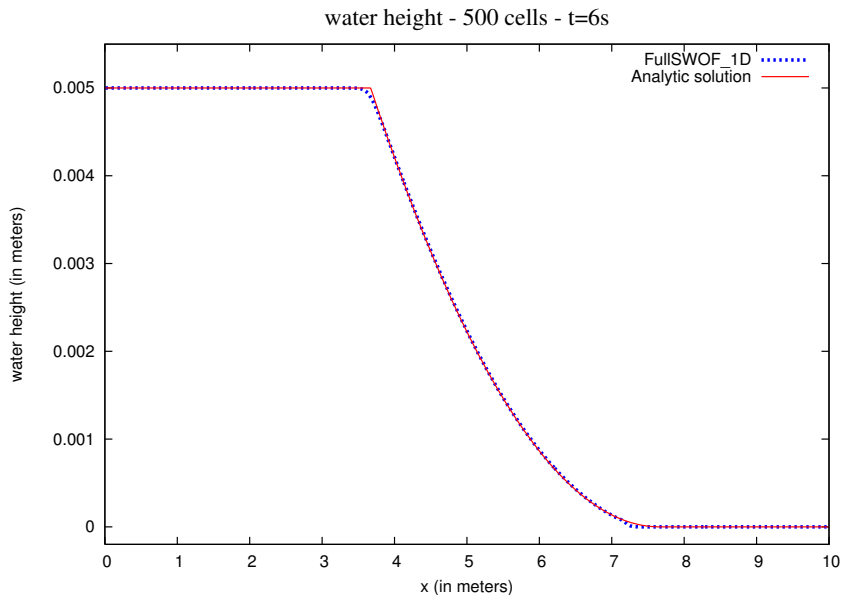


Figure 23: Results of FullSWOF_1D for a dam break on a dry domain without friction

the surface is wet up to $x = 7.6$ m according to the analytic solution, while FullSWOF_1D predicts a dry surface for $x > 7.3$ m. It shows the water front predicted by FullSWOF_1D moves a bit too slowly. This difference can be due to the degeneracy of the system for vanishing water height. For $x > 7.6$ m, both the analytic solution and FullSWOF_1D result give a null water height: on dry areas, FullSWOF_1D does not predict positive or negative water heights, and the dry-to-wet transition does not show any spurious point, contrarily to other codes.

Dressler’s dam break with friction The parameters of the Dressler’s dam break are recalled in Section 4.1.3. For FullSWOF_1D, we take a Darcy-Weisbach’s friction law with a coefficient equal to 0.04905. The results are given on Figure 24.

On this example, one can note first that, as in the other dam breaks, FullSWOF_1D smooths the solution at sharp angles. But there is also a difference at the wet/dry interface: the friction seems to be underestimated compared to the analytic solution.

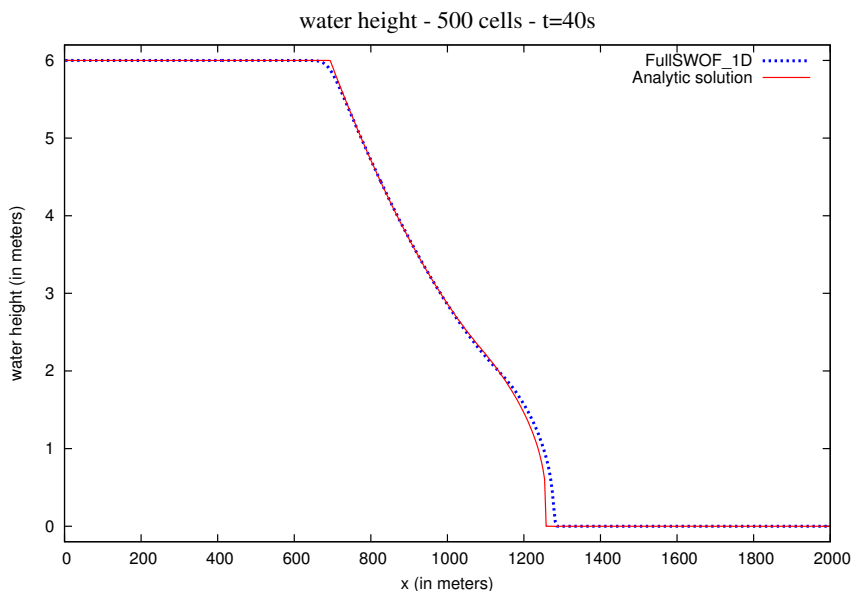


Figure 24: Results of FullSWOF_1D for Dressler’s break with friction

6.2.8 Oscillations

Planar surface in a parabola without friction The planar surface in a parabola without friction is a one dimensional Thacker’s case, see Section 4.2.1. The results are given on Figure 25, after 5 periods.

After oscillating to the right and then to the left five times, the water surface recovers its initial position (as there is no friction). The approximate solution matches well the analytic solution, there is no peak at the wet / dry transitions.

Planar surface in a parabola with friction For Sampson’s test case, see Section 4.2.3, a linear friction is added. However, up to now, FullSWOF cannot model this linear friction. So, we plotted on Figure 26 only the analytic solution.

6.3 Examples in two dimensions

We now consider the results given by the two-dimensional software FullSWOF_2D.

6.3.1 Oscillations

Radially-symmetrical paraboloid This first two-dimensional case is the radially-symmetrical Thacker’s case in a paraboloid, see Section 4.2.2. We run FullSWOF_2D with the corresponding parameters, and we plotted a cross section of the results for $y = 2.02$ m after three periods on Figure 27.

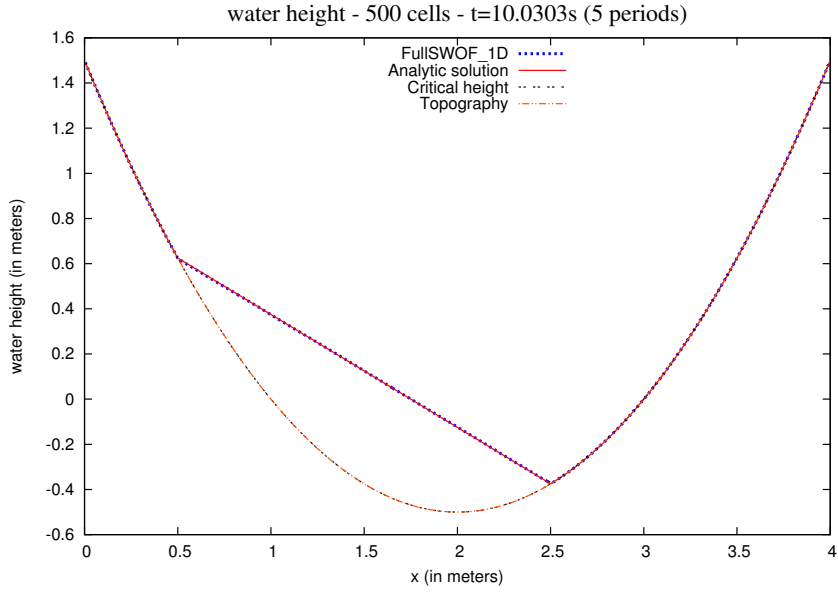


Figure 25: Results of FullSWOF_1D for Thacker's solution

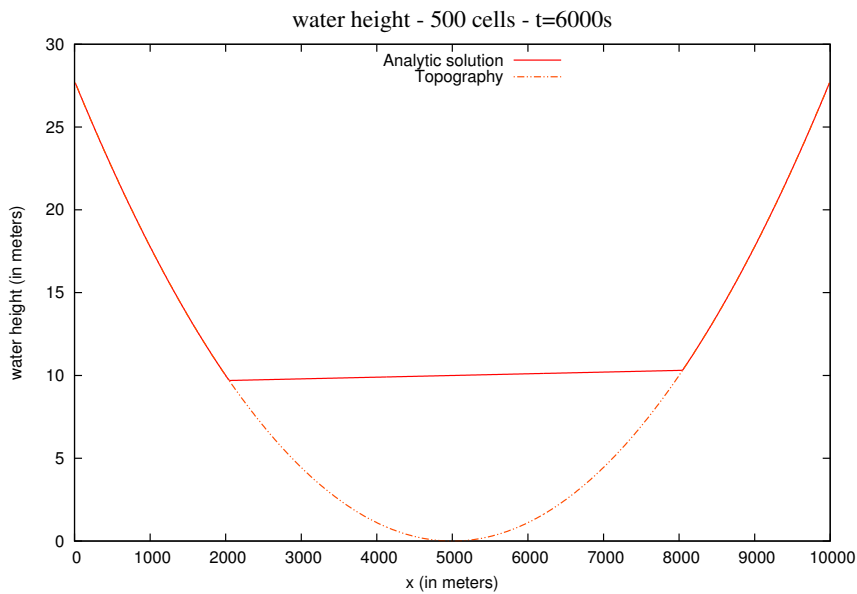


Figure 26: Analytic solution for Sampson's solution

The approximate solution given by FullSWOF_2D corresponds to the analytic solution, the numerical diffusion is not visible, and the wet / dry transitions are well treated.

Planar surface in a paraboloid In the case of Thacker's planar surface in a paraboloid (see Section 4.2.2), FullSWOF_2D was run for three periods on a domain of $[0 \text{ m}; 4 \text{ m}] \times [0 \text{ m}; 4 \text{ m}]$ with 500×500 cells. To analyse the performances of FullSWOF_2D, we consider a cross section along x (Figure 28).

water height - 100*100 cells - t=6.72855s (3 periods)

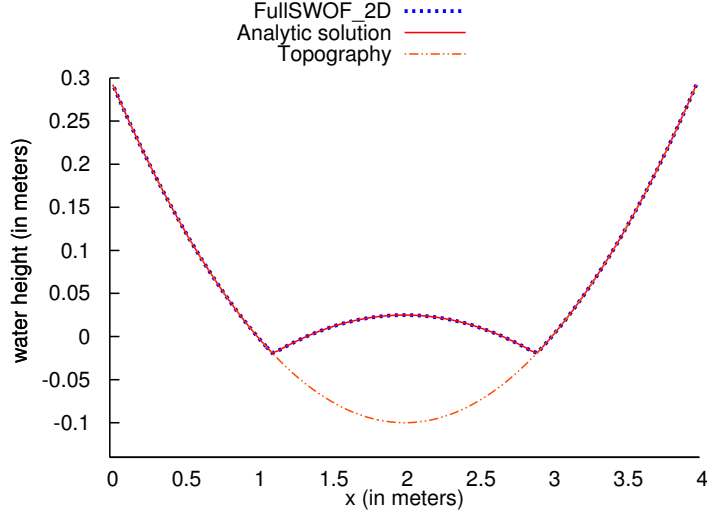


Figure 27: Cross section along x of FullSWOF_2D result for the radially-symmetrical Thacker’s case in a paraboloid

Overall, FullSWOF_2D produces a good approximation of the analytic solution: while the maximum water height is 0.1 m, errors are in the domain $[-1.55 \times 10^{-3} \text{ m}; +7.65 \times 10^{-4} \text{ m}]$. At the wet-dry transition located at $x = 1.5 \text{ m}$, FullSWOF_2D overestimates the water height by about $+6 \times 10^{-4} \text{ m}$ and, on a single cell, FullSWOF_2D predicts water while the analytic solution gives a dry surface. Close to $x = 1.5 \text{ m}$, the overestimation of the water height is up to +43%, but decreases quickly and is always less than +5% for $x > 1.57 \text{ m}$. The overestimation persists up to $x = 2.65 \text{ m}$ and then becomes an underestimation. The underestimation tends to grow up to the wet-dry transition at $x = 3.5 \text{ m}$ (reaching -5% at $x = 3.38 \text{ m}$). Starting exactly at $x = 3.5 \text{ m}$ (and on the same cell) both FullSWOF_2D and the analytic solution predict no water. However, on the cell just before, FullSWOF_2D underestimates the water height by -97% (but at this point, the water height given by the analytic solution is only $1.6 \times 10^{-3} \text{ m}$).

6.3.2 Mac Donald pseudo-2D solutions

We consider two Mac Donald pseudo-2D solutions. Since FullSWOF_2D does not solve the pseudo-2D Shallow-Water system but the full Shallow-Water system in 2D (1), more significant differences are expected. In both cases, FullSWOF_2D was run long enough to reach steady-state.

Subcritical flow in a short domain This test case is detailed in Section 3.5.1. As the results of FullSWOF_2D are not really relevant, we only plot the analytic solution on Figure 29.

Supercritical flow in a short domain The case of a supercritical flow in a short domain (Section 3.5.2) is computed with 400×201 cells on the domain $[0 \text{ m}; 200 \text{ m}] \times [0 \text{ m}; 9.589575 \text{ m}]$, with the topography

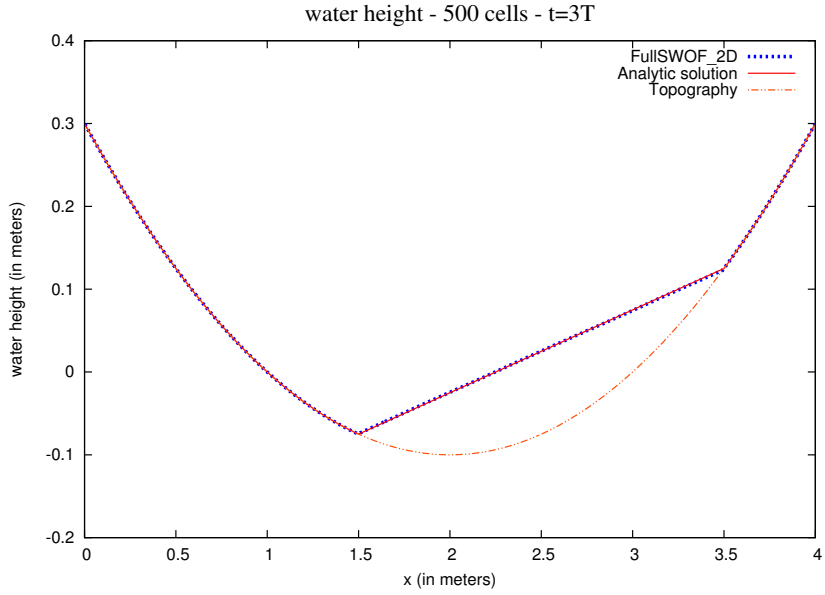


Figure 28: Cross section along x of FullSWOF_2D result for Thacker’s planar surface in a paraboloid

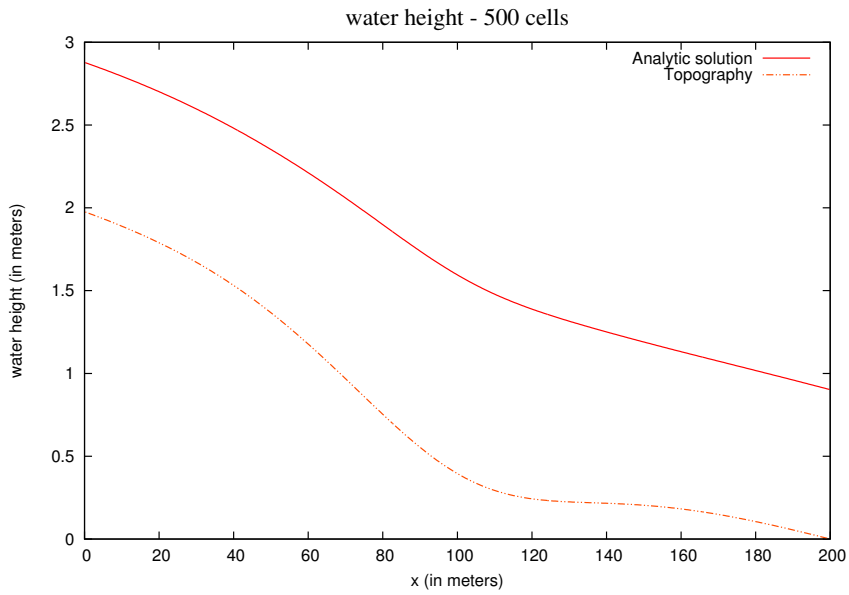


Figure 29: Analytic solution for Mac Donald’s subcritical flow with the B_1 shape for the bottom

B_1 . The y -averaged result of FullSWOF_2D differs from the analytic solution mainly around $x = 100$ m (Figure 30), with an underestimation of the water height of up to -0.018 m (-11.85%). This underestimation occurs on the whole domain and gets closer to zero near both the upper and lower boundaries.

Smooth transition in a short domain The shape of the bottom is still B_1 , but there is a smooth transition, see section 3.5.3. The analytic solution is depicted in Figure 31.

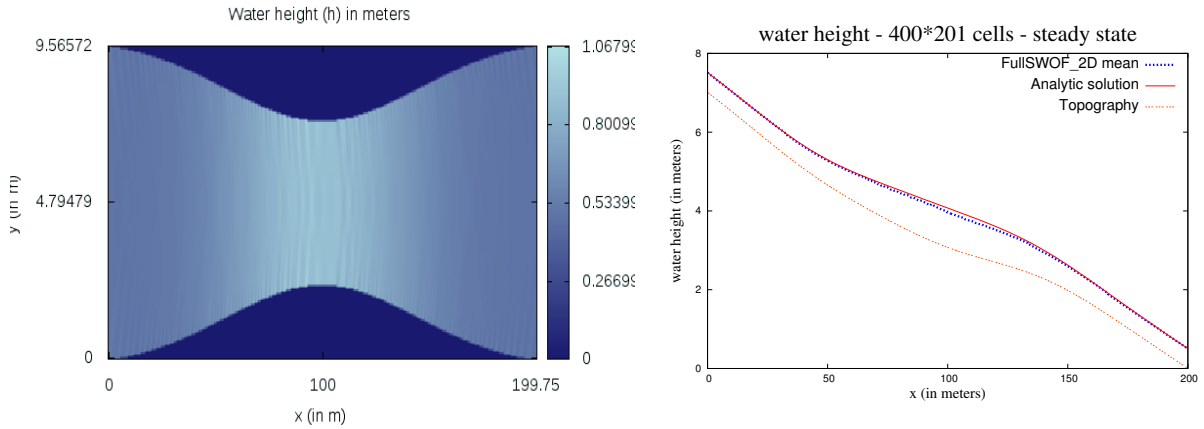


Figure 30: Results of FullSWOF_2D for the Mac Donald pseudo-2D supercritical solution in a short domain

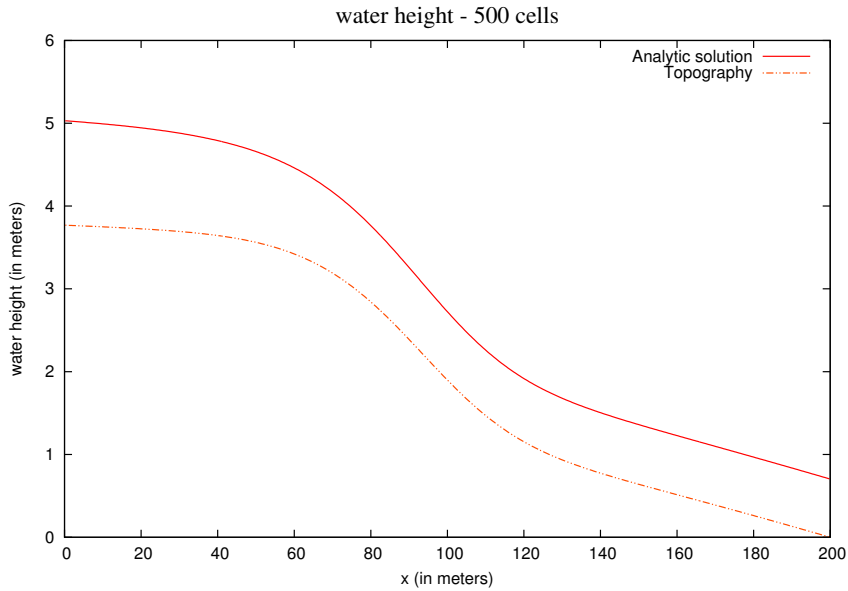


Figure 31: Analytic solution for Mac Donald's smooth transition case with the B_1 shape for the bottom

Hydraulic jump in a short domain In Section 3.5.4, we give a fourth example of Mac Donald's solution, with an hydraulic jump. This solution is plotted on Figure 32: the jump is located around $x = 120$ m.

Subcritical flow in a long domain The case of a subcritical flow in a long domain (Section 3.5.5) is computed with 800×201 cells on the domain $[0 \text{ m}; 400 \text{ m}] \times [0 \text{ m}; 9.98067 \text{ m}]$, with the topography B_2 . Comparison between the y -averaged FullSWOF_2D result and the analytic solution shows clear differences (Figure 33), even if the overall shape of the free surface given by FullSWOF_2D matches the analytic solution. FullSWOF_2D underestimates the water height on most of the domain. This difference can be up to -0.088 m (-8.8%) at $x = 66$ m. FullSWOF_2D overestimates water height for $x > 297$ m and this overestimation can reach up to $+0.04$ m ($+4.1\%$) at $x = 334$ m.

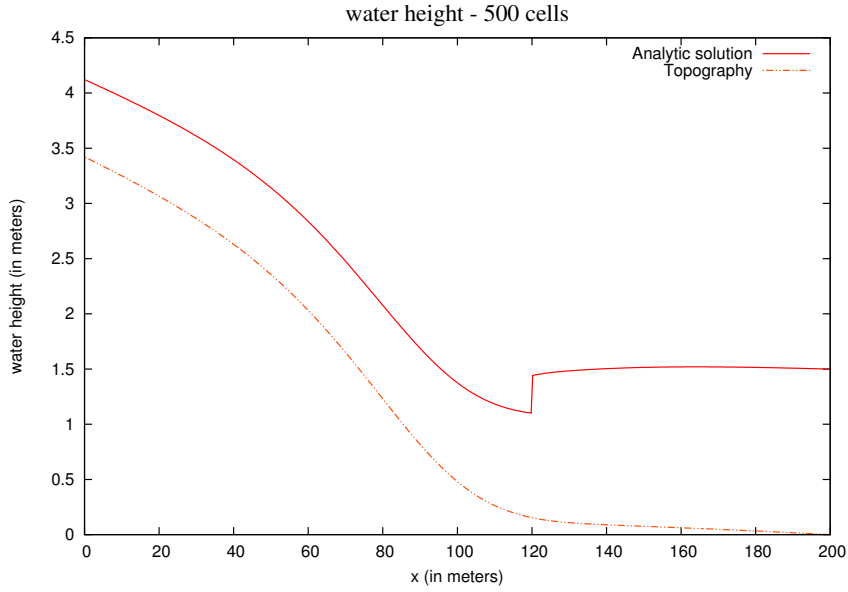


Figure 32: Analytic solution for Mac Donald’s hydraulic jump case with the B_1 shape for the bottom

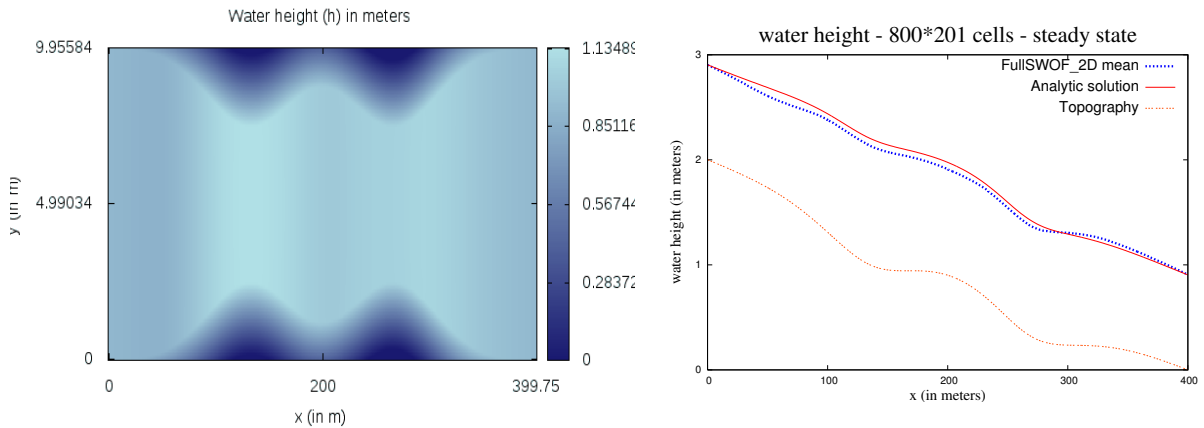


Figure 33: Result of FullSWOF_2D for the Mac Donald pseudo-2D subcritical solution in a long domain

Smooth transition followed by a hydraulic jump in a long domain The second analytic solution for the B_2 topography is described in Section 3.5.6 and the results are plotted on Figure 34: there is a smooth transition followed by an hydraulic jump located at about $x = 120$ m.

Acknowledgments

The authors wish to thank Valerio Caleffi and Anne-Céline Boulanger for their collaboration. This study is part of the ANR METHODE granted by the French National Agency for Research ANR-07-BLAN-0232.

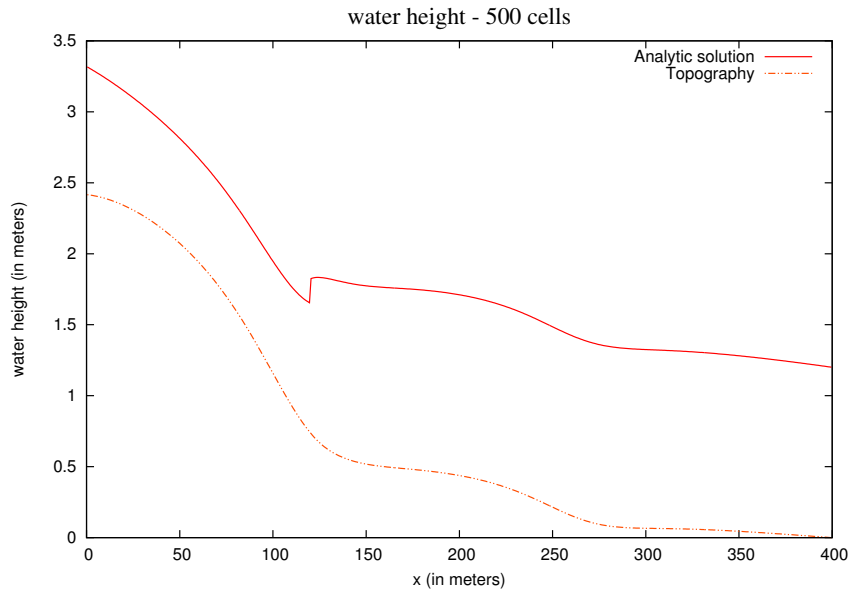


Figure 34: Analytic solution for Mac Donald’s smooth transition and hydraulic jump case with the B_2 shape for the bottom

References

- [1] Francisco Alcrudo and Elena Gil. The Malpasset dam break case study. In *Proceedings of the 4th Concerted Action on Dambreak Modelling Workshop*, pages 95–109, Zaragoza, Spain, November 1999.
- [2] E. Audusse, F. Bouchut, M.-O. Bristeau, R. Klein, and B. Perthame. A fast and stable well-balanced scheme with hydrostatic reconstruction for shallow water flows. *SIAM Journal on Scientific Computing*, 25(6):2050–2065, 2004.
- [3] F. K. Ball. Some general theorems concerning the finite motion of a shallow rotating liquid lying on a paraboloid. *Journal of Fluid Mechanics*, 17(2):240–256, 1963.
- [4] Adhémar Jean-Claude Barré de Saint Venant. Théorie du mouvement non-permanent des eaux, avec application aux crues des rivières et à l’introduction des marées dans leur lit. *Comptes Rendus de l’Académie des Sciences*, 73:147–154, 1871.
- [5] Alfredo Bermúdez and Ma Elena Vázquez. Upwind methods for hyperbolic conservation laws with source terms. *Computers and Fluids*, 23(8):1049–1071, 1994.
- [6] A. G. L. Borthwick, S. Cruz León, and J. Józsa. The shallow flow equations solved on adaptative quadtree grids. *International Journal for Numerical Methods in Fluids*, 37(6):691–719, November 2001.
- [7] F. Bouchut. *Nonlinear stability of finite volume methods for hyperbolic conservation laws, and well-balanced schemes for sources*, volume 4 of *Frontiers in Mathematics*. Birkhäuser Verlag, Basel - Boston - Berlin, 2004.
- [8] M.-O. Bristeau and B. Coussin. Boundary conditions for the shallow water equations solved by kinetic schemes. Technical Report RR-4282, INRIA, October 2001.

- [9] J. Burguete and P. García-Navarro. Implicit schemes with large time step for non-linear equations: application to river flow hydraulics. *International Journal for Numerical Methods in Fluids*, 46(6):607–636, October 2004.
- [10] V. Caleffi, A. Valiani, and A. Zanni. Finite volume method for simulating extreme flood events in natural channels. *Journal of Hydraulic Research*, 41(2):167–177, 2003.
- [11] G. F. Carrier and H. P. Greenspan. Water waves of finite amplitude on a sloping beach. *Journal of Fluid Mechanics*, 4(1):97–109, 1958.
- [12] Hubert Chanson. Applications of the Saint-Venant equations and method of characteristics to the dam break wave problem. Technical Report CH55-05, Department of Civil Engineering, The University of Queensland, Brisbane, Australia, May 2005.
- [13] Hubert Chanson. Solutions analytiques de l’onde de rupture de barrage sur plan horizontal et incliné. *La Houille Blanche*, 3:76–86, 2006.
- [14] V. T. Chow. *Open-channel hydraulics*. McGraw-Hill, New-York, USA, 1959.
- [15] O. Delestre. Ecriture d’un code C++ pour la simulation en hydrologie. Master’s thesis, Université d’Orléans, Orléans, France, September 2008.
- [16] Olivier Delestre. *Simulation du ruissellement d’eau de pluie sur des surfaces agricoles*. PhD thesis, Université d’Orléans, Orléans, France, July 2010.
- [17] Olivier Delestre, Stéphane Cordier, François James, and Frédéric Darboux. Simulation of rain-water overland-flow. In E. Tadmor, J.-G. Liu, and A. Tzavaras, editors, *Proceedings of the 12th International Conference on Hyperbolic Problems*, volume 67 of *Proceedings of Symposia in Applied Mathematics*, pages 537–546, University of Maryland, College Park (USA), 2009. Amer. Math. Soc.
- [18] Olivier Delestre and Pierre-Yves Lagrée. A “well balanced” finite volume scheme for blood flow simulation. submitted, 2011.
- [19] Olivier Delestre and Fabien Marche. A numerical scheme for a viscous shallow water model with friction. *Journal of Scientific Computing*, 48(1-3):41–51, 2011.
- [20] Robert F. Dressler. Hydraulic resistance effect upon the dam-break functions. *Journal of Research of the National Bureau of Standards*, 49(3):217–225, September 1952.
- [21] Robert F. Dressler. Comparison of theories and experiments for the hydraulic dam-break wave. In *Assemblée générale de Rome — Comptes-Rendus et Rapports de la Commission des Eaux de Surface*, volume 38, pages 319–328. Union Géodésique et Géophysique Internationale - Association Internationale d’Hydrologie Scientifique, Association Internationale d’Hydrologie, 1954.
- [22] M. Esteves, X. Faucher, S. Galle, and M. Vauclin. Overland flow and infiltration modelling for small plots during unsteady rain: numerical results versus observed values. *Journal of Hydrology*, 228(3-4):265–282, March 2000.
- [23] D. L. George. *Finite volume methods and adaptive refinement for tsunami propagation and inundation*. PhD thesis, University of Washington, USA, 2006.
- [24] Edwige Godlewski and Pierre-Arnaud Raviart. *Numerical approximations of hyperbolic systems of conservation laws*, volume 118 of *Applied Mathematical Sciences*. Springer-Verlag, New York, 1996.
- [25] N. Goutal and F. Maurel. A finite volume solver for 1D shallow-water equations applied to an actual river. *International Journal for Numerical Methods in Fluids*, 38(1):1–19, January 2002.

- [26] N. Goutal and J. Sainte-Marie. A kinetic interpretation of the section-averaged Saint-Venant system for natural river hydraulics. *International Journal for Numerical Methods in Fluids*, 67(7):914–938, 2011.
- [27] Nicole Goutal and François Maurel. Proceedings of the 2nd workshop on dam-break wave simulation. Technical Report HE-43/97/016/B, Electricité de France, Direction des études et recherches, 1997.
- [28] J. M. Greenberg and A. Y. LeRoux. A well-balanced scheme for the numerical processing of source terms in hyperbolic equations. *SIAM Journal on Numerical Analysis*, 33(1):1–16, 1996.
- [29] Amiram Harten, Peter D. Lax, and Bram van Leer. On upstream differencing and Godunov-type schemes for hyperbolic conservation laws. *SIAM Review*, 25(1):35–61, 1983.
- [30] F. M. Henderson. *Open channel flow*. Civil engineering. MacMillan, New York, nordby, g. edition, 1966.
- [31] J.-M. Hervouet. *Hydrodynamics of Free Surface Flows: Modelling with the Finite Element Method*. Wiley, April 2007.
- [32] David D. Houghton and Akira Kasahara. Nonlinear shallow fluid flow over an isolated ridge. *Communications on Pure and Applied Mathematics*, 21:1–23, January 1968.
- [33] D.-H. Kim, Y.-S. Cho, and Y.-K. Yi. Propagation and run-up of nearshore tsunamis with HLLC approximate Riemann solver. *Ocean Engineering*, 34(8–9):1164–1173, June 2007.
- [34] R. J. LeVeque. *Finite volume methods for hyperbolic problems*. Number 31 in Cambridge Texts in Applied Mathematics. Cambridge University Press, August 2002.
- [35] I. MacDonald. *Analysis and computation of steady open channel flow*. PhD thesis, University of Reading — Department of Mathematics, September 1996.
- [36] I. MacDonald, M. J. Baines, N. K. Nichols, and P. G. Samuels. Analytic benchmark solutions for open-channel flows. *Journal of Hydraulic Engineering*, 123(11):1041–1045, November 1997.
- [37] F. Marche. *Theoretical and numerical study of shallow water models. Applications to nearshore hydrodynamics*. PhD thesis, Laboratoire de mathématiques appliquées - Université de Bordeaux 1, Bordeaux, France, December 2005.
- [38] F. Marche. Derivation of a new two-dimensional viscous shallow water model with varying topography, bottom friction and capillary effects. *European Journal of Mechanics B/Fluids*, 26(1):49–63, 2007.
- [39] H. Matsutomi. Dam-break flow over a uniformly sloping bottom. *Journal of Hydraulics, Coastal and Environmental Engineering. Japan Society of Civil Engineers*, 726/II-62:151–156, February 2003.
- [40] J. W. Miles and F. K. Ball. On free-surface oscillations in a rotating paraboloid. *Journal of Fluid Mechanics*, 17(2):257–266, 1963.
- [41] Stéphane Popinet. Quadtree-adaptative tsunami modelling. *Ocean Dynamics*, 61(9):1261–1285, 2011.
- [42] A. Ritter. Die Fortpflanzung der Wasserwellen. *Zeitschrift des Vereines Deutscher Ingenieure*, 36(33):947–954, August 1892.
- [43] Joe Sampson, Alan Easton, and Manmohan Singh. Moving boundary shallow water flow above parabolic bottom topography. In Andrew Stacey, Bill Blyth, John Shepherd, and A. J. Roberts, editors, *Proceedings of the 7th Biennial Engineering Mathematics and Applications Conference, EMAC-2005*, volume 47 of *ANZIAM Journal*, pages C373–C387. Australian Mathematical Society, October 2006.

- [44] Joe Sampson, Alan Easton, and Manmohan Singh. Moving boundary shallow water flow in a region with quadratic bathymetry. In Geoffrey N. Mercer and A. J. Roberts, editors, *Proceedings of the 8th Biennial Engineering Mathematics and Applications Conference, EMAC-2007*, volume 49 of *ANZIAM Journal*, pages C666–C680. Australian Mathematical Society, July 2008.
- [45] Gary A. Sod. A survey of several finite difference methods for systems of nonlinear hyperbolic conservation laws. *Journal of Computational Physics*, 27(1):1–31, April 1978.
- [46] J. J. Stoker. *Water Waves: The Mathematical Theory with Applications*, volume 4 of *Pure and Applied Mathematics*. Interscience Publishers, New York, USA, 1957.
- [47] L. Tatard, O. Planchon, J. Wainwright, G. Nord, D. Favis-Mortlock, N. Silvera, O. Ribolzi, M. Esteves, and Chi-hua Huang. Measurement and modelling of high-resolution flow-velocity data under simulated rainfall on a low-slope sandy soil. *Journal of Hydrology*, 348(1–2):1–12, January 2008.
- [48] William Carlisle Thacker. Some exact solutions to the nonlinear shallow-water wave equations. *Journal of Fluid Mechanics*, 107:499–508, 1981.
- [49] E. F. Toro. *Riemann solvers and numerical methods for fluid dynamics. A practical introduction*. Springer-Verlag, Berlin and New York), 3 edition, 2009.
- [50] A. Valiani, V. Caleffi, and A. Zanni. Finite volume scheme for 2D shallow-water equations. Application to the Malpasset dam-break. In *Proceedings of the 4th Concerted Action on Dambreak Modelling Workshop*, pages 63–94, Zaragoza, Spain, November 1999.
- [51] A. Valiani, V. Caleffi, and A. Zanni. Case study: Malpasset dam-break simulation using a two-dimensional finite volume method. *Journal of Hydraulic Engineering*, 128(5):460–472, May 2002.
- [52] Bram van Leer. Towards the ultimate conservative difference scheme. V. A second-order sequel to Godunov’s method. *Journal of Computational Physics*, 32(1):101–136, July 1979.
- [53] Thi Ngoc Tuoi Vo. One dimensional Saint-Venant system. Master’s thesis, Université d’Orléans, France, June 2008.
- [54] G. B. Whitham. The effects of hydraulic resistance in the dam-break problem. *Proceedings of the Royal Society of London, Ser. A.*, 227(1170):399–407, January 1955.
- [55] Chao Wu. Ritter’s solution of dam-breaking wave in trapezoid cross-section channel. *Advances in Hydrodynamics*, 1(2):82–88, December 1986.
- [56] J. G. Zhou and P. K. Stansby. 2D shallow water flow model for the hydraulic jump. *International Journal for Numerical Methods in Fluids*, 29(4):375–387, February 1999.